



Ministry of Higher Education and Scientific Research
University of Al Iraqia
College of Engineering
Computer Engineering Department



A SOFT COMPUTING MODEL FOR IMAGE REGISTRATION AND CLASSIFICATION: BRAIN TUMORS CASE STUDY

A Thesis

**Submitted to College of Engineering of Al Iraqi University
in Partial Fulfillment of the Requirements for the Degree of
Master of Science in Department Computer Engineering.**

By

ISRAA YARUB YOUSSEF ABDEL-HUSSEIN

Supervised By

Asst.Prof.Dr Tayseer S. Atia

Asst.Prof.Dr Mushtaq A. Ali

2021 A.D.

1442 A.H

Supervisors' Certification

We certify that this project entitled " A Soft Computing Model For Image Registration And Classification: Brain Tumors Case Study " was prepared by" Israa Yarub Youssef "under my supervision at Al-Iraqia University / College of Engineering in partial fulfillmentAz of the requirements for the degree of Master of Science in Computer Engineering.

Signature:

Name: Tayseer Salman Atia

(Supervisor)

Date: / /2021

Signature:

Name: Mushtaq Ahmed Ali

(Supervisor)

Date: / /2021

Signature:

Name: Asst.Prof.Dr. Mudhafar Hussein Ali

(Head of Department)

Date: / / 2021

Certificate

We certify, as an examining committee, that we have read this project entitled "(A Soft Computing Model For Image Registration And Classification: Brain Tumors Case Study)" , examined the student (Israa Yarub Youssef) in its content and found it meets the standard of graduation project for the degree of Master of Science in Computer Engineering.

Signature:

Name: Asst.Prof.Dr. Tayseer Salman Atia

(Supervisor)

Date: / / 2021

Signature:

Name: Asst.Prof.Dr. Mushtaq Ahmed Ali

(Supervisor)

Date: / / 2021

Signature:

Name: Dr. Omar Hussein Salman

(Member)

Date: / / 2021

Signature:

Name: Asst.Prof.Dr. Muna Hadi Saleh

(Member)

Date: / / 2021

Signature:

Name: Asst.Prof.Dr. Baraa Munqith Albaker

(Chairman)

Date: / / 2021

Approval of the college of Engineering

Signature:

Name: Asst.Prof.Dr. Muwafaq Shyaa Alwan

(Dean)

Date: / / 2021

Abstract

Acquiring images from different viewpoints, corners, and times raise the problem of incomplete image details. They are not useful for further medical analysis such as diagnosis. The medical image registration techniques overcome this problem by constructing a complementary image from an incomplete set of images by finding the best matching or transformation between two images. The results of the IR (Image Registration) stage influence the accuracy of the image classification stage.

In this thesis, The system consists of two parts, in the first part is a MIR approach is developed. It combines the approaches of matching-based and parameter-based for a robust registration process and reasonable time. included A GA(Genetic Algorithm) optimizer model (from parameter-based) incorporates wavelet(Haar) and fusion(max , average) techniques(from matching-based). Furthermore, for proving the accuracy of the developed MIR approach, the output is analyzed by a Fuzzy-PNN classifier model. For the implementation which represents the second part of the system, a 2D MRI(Magnetic Resonance Imaging) is employed in the registration technique for the classification and diagnosis of brain tumors. The proposed classification system is automated through a transmission model. Which consists of Arduino and GSM card where decisions(normal or ubnormal) sent via the cellular network to the patient's phone.

The implementation results for the developed MIR indicated that it has a higher entropy (robust measure) (1.101, 4.789) compared to an existing method. Also, the Fuzzy-PNN classifier has a high average



'accuracy rate' compared to other existing methods in the literature, where the average accuracy is 100% (training70%, testing30%) using PNN with a reasonable time. It concludes that hybrid systems combine the best feature between two systems and perform better than each one alone. Based on that conclusion, it is recommended to use the proposed system to automate the registration and classification process add to gaining the benefit of reducing diagnosis error when classified manually.

List of Contents

Contents	Page
Abstract	I
List of Contents	III
List of Abbreviations	VII
List of Table	X
List of Figures	XI

Chapter 1: General Introduction

1.1	General Introduction	1
1.2	Motivation	3
1.3	Problem Statement	3
1.4	Aim and Objective	4
1.5	Contribution	5
1.6	Related Works	6
1.7	Thesis organization	15

Chapter 2: Theoretical Background

2.1	Introduction	16
2.2	Image Registration	16
2.3	Image Registration Approach	16
2.3.1	Medical Image	18
2.3.2	Feature Extraction	23
2.3.2.1	Local Binary Patterns (LBP)	23
2.3.2.2	Speeded up Robust Feature (SURF)	24
2.3.2.3	Binary Robust Invariant Scalable Keypoints (BRISK)	25
2.3.2.4	Harris Detector	26
2.3.2.5	Minimum Eigenvalue Algorithm (Min Eigen)	28
2.4	Image Enhancement	30
2.5	Image Fusion	31
2.5.1	Discrete Wavelet Transform	34
2.6	The Entropy	37
2.7	Soft Computing	38
2.7.1	Fuzzy Logic	39
2.7.2	Neural Network (NN)	43
2.7.2.1	Details of PNN	44
2.7.3	Genetic Algorithm(GA)	47
2.8	Performance Measurement	51
2.9	Transmission Model(Arduino and GSM)	53

Chapter 3: A SOFT COMPUTING MODEL FOR IMAGE REGISTRATION AND CLASSIFICATION

3.1	Introduction	56
3.2	The Proposed Automatic Classification System	56
3.2.1	System Input	58
3.2.2	Medical Image Registration Model	58
3.2.2.1	Image Enhancement	58
3.2.2.2	GA Optimizer	59
3.2.3	Fuzzy- PNN classifier Model	62
3.2.3.1	Features Extraction	62
3.2.3.2	Fuzzy Inference System	64
3.2.3.3	PNN Classifier	70
3.2.4	Transmission Model	74

Chapter 4: IMPLEMENTATION RESULT AND DISCUSSION

4.1	Introduction	76
4.2	Proposed System Implementation	76
4.3	Proposed System Implementation Results	79
4.3.1	Medical Image Registration Model	79



4.3.1.1	Image Enhancement	79
4.3.1.2	GA Optimizer Implementation	80
4.3.2	Fuzzy-PNN Classifier Model Implementation	83
4.3.2.1	Features Extraction Result	83
4.3.2.2	The FIS Implementation	87
4.3.2.3	PNN Classifier Implementation	95
4.3.3	Transmission Model Implementation:	98
4.4	Evaluation	98
4.5	Limitations	100

Chapter 5: Conclusion and Suggestion for Future Work

5.1	Introduction	101
5.2	Conclusion	101
5.3	Suggestion for future works	102

List of Abbreviations

AI	Artificial Intelligence
AUC	Area under the curve
BOA	Bisector of Area
BRISK	Binary Robust Invariant Scalable Keypoints
COS	Center of Sums
COG	Center of Gravity
COA	Centroid of Area
CP	Control Center
CNN	Convolutional Neural Networks
CT	Computed Tomography
DL	Deep Learning
DWT	Discrete Wavelet Transformation
DTCWT	Dual tree Complex Wavelet Transform
EC	Evolutionary Computation
FB	Filter Bank
FIS	Fuzzy Inference System
FP	False Positive
FN	False Negative
FOM	First of Maxima Method
FMRI	Functional Magnetic Resonance Imaging
GA	Genetic Algorithm
GLCM	Gray Level Co-occurrence Matrix
GPRS	General Packet Radio Service

GSM	Global System for Mobile
HPF	High-Pass Filtering
HRPI	High-Resolution Panchromatic Image
HRMI	High-Resolution Multispectral Images
HOG	Histogram of Oriented Gradients
IR	Image Registration
ICP	Iterative Closest Point
IT	Image Right
IoT	Internet of Things
LRMI	Low-Resolution Multispectral Image
LRPI	Low-Resolution Panchromatic Image
LOM	Last of Maxima Method
LBP	Local Binary Patterns
MIR	Medical Image Registration
MRI	Magnetic Resonance Imaging
MAP	Maximum a Posteriori
MOM	Mean of Maxima Method
MFs	Membership Functions
MI	Medical Image
Min Eigen	Minimum Eigenvalue Algorithm
NN	Neural Network
PC	Personal Computer
PSNR	Peak Signal-to-Noise Ratio
PET	Positron Emission Tomography
PCA	Principal Component Analysis
PNN	Probabilistic Neural Network
RNN	Recurrent Neural Network

RMSE	Root Mean Square Error
SIM	Subscriber Identification Module
SPECT	Single-Photon Emission Computed Tomography
SURF	Speeded up Robust Feature
2D	Two Dimension
TDMA	Time Division Multiple Access
TP	True Positive
TN	True Negative

List of Tables

Table	Title	Page
(1.1)	List of Related Works(IR)	10
(1.2)	List of Related Works(Automatic Detection)	12
(2.1)	Membership Function	41
(2.2)	Types of Fuzzy Implication	42
(2.3)	Type of Defuzzification	43
(2.4)	Confusion Matrix	51
(2.5)	Classification Performance Measurement	53
(2.6)	The Types of Arduino	54
(4.1)	Hardware Experimental	77
(4.2)	Software Experimental	78
(4.3)	GA Operation for 1 st Generation	80
(4.4)	The Original Image and Its Divisions	83
(4.5)	The Extract Features from two Parts of the Image	85
(4.6)	Feature Extraction Output	88
(4.7)	The Features Extraction by Rule Result	94
(4.8)	The Number of Features Extracted in Fuzzy Rule	95
(4.9)	Training /Testing Percentage with Accuracy	96
(4.10)	Smoothing Parameter value impact	96
(4.11)	Confusion Matrix for Classification phase	97
(4.12)	The Performance Measures for Classification	97



	Phase	
(4.13)	The Entropy of DWT& Fusion	99
(4.14)	The PNN and other Neural Network Accuracy	100

List of Figures

Figure	Title	Page
(2.1)	Image Registration	18
(2.2)	Picture of a CT Scanner	19
(2.3)	MRI Scan	20
(2.4)	Combination of a CT Scan and a PET Scan	21
(2.5)	An Ultrasounds	22
(2.6)	Diagram of How an x-ray Scanner Works	22
(2.7)	Harris Corner Detector	28
(2.8)	Min Eigen	29
(2.9)	The Feature Extraction Stage	29
(2.10)	The Fusion Image Stage	31
(2.11)	Discrete Wavelet Transform	34
(2.12)	DWT in Image Processing	35
(2.13)	Basic Soft Computing Diagram	39
(2.14)	Fuzzy Inference System Diagram	41

(2.15)	The Most Famous Type of Neural Network	44
(2.16)	Architecture of PNN	47
(2.17)	Flowchart of Basic Genetic Algorithm Iteration	48
(2.18)	Crossover and Mutation Operator	51
(2.19)	Types of Arduino Boards	54
(3.1)	Proposed Diagnosis System	57
(3.2)	Diagram of the Crossover	60
(3.3)	Membership Function of the Fuzzy Sets	64
(3.4)	Output of the Fuzzy Set	65
(3.5)	The Structure of PNN	72
(3.6)	Diagram of Transmission Model	74
(4.1)	The Deployment Diagram for the Proposed System	76
(4.2)	The Samples of data set(a,b,c,d,e,f,g,h,I, and j) Samples of Different Medical Image	78
(4.3)	Image Enhancement Results (a) Before Enhance and (b) After Enhance	79
(4.4)	FIS workflow	87
(4.5)	Part of the Inference Rule(Larsen)	89
(4.6)	Part of the Inference Rule(Mamdani)	90
(4.7)	Part of the Inference Rule(Zadeh)	91
(4.8)	Part of the Inference Rule(DienesRescher)	92
(4.9)	Part of the Inference Rule(Lukasiewicz)	93
(4.10)	Connecting Arduino with computer and GSM	98

CHAPTER ONE

INTRODUCTION

1.1 General Introduction

Currently, medical imaging systems have a crucial role in the clinical workflow due to their ability to reflect anatomical and physiological features which are not otherwise available for inspection[1]. Medical image technology uses different concepts to quantify the spatial distributions of the physical characteristics of humans and help understand complex or unusual diseases [2].

The method of integrating complementary information from two or more medical images acquired by medical device for a certain organ into a single composite image is more informative [3]. The number of available modalities and the volume of data in the medical image makes it very difficult to use explicitly at various levels of complementary data[4]. Moreover, each modality offers a limited amount of knowledge, and very often two or more modes of the same patient are employed to get the sensed material well understood[ref]. IR(Image Registration) overcome this problem by finding a match or transformation between two images generated from the same system or different system, at the same time or not, and from a different viewpoint[5].

IR approaches are classified as matching-based or parameter-based[6]. In the first one, the best matching between two images has to

be found through (preprocessing, feature extraction, matching, and transformation) [5]. However, this approach lacks robustness and gets stuck in local minima[7]. While the second uses a geometric transformation to find the parameter that can best align two images using an optimizer which also considers the challenging problem in this approach[8].

Applications of image registration in the medical field include fusion of anatomical images from Computerized Tomography (CT) or Magnetic Resonance Imaging (MRI) images[9]. Complementary image construction by combining data from different images to obtain complete information about the patient[10]. Complementary image assesses monitoring tumor growth, treatment verification comparison of the patient's data with anatomical atlases[11].

In this context, brain cancers are the most common and aggressive disease, leading to a very short life expectancy in their highest grade[12]. MRI image is the appropriate type to evaluate the tumor in the brain, lung, liver, breast, prostate[13]. In this thesis, MRI images are used to diagnose a tumor in the brain. However, the huge amount of data generated by MRI scans thwarts manual classification of tumor vs. non-tumor at a particular time. But it has some limitation (i.e) accurate quantitative measurements is provided for the limited number of images[14]. Hence a trusted image registration is essential to automatic classification schemes and prevents the death rate of humans. The automatic brain tumor classification is a very challenging task in large spatial and structural variability of the surrounding region of brain tumor.

Soft computing paradigms (GA, FL, ANN) play a vital role in MIR(Medical Image Registration) and classification, where the GA is employed as an optimizer in the MIR process, and the ANN model is applied in classification and diagnosis. Finally, fuzzy logic offers the ability to work with uncertain or uncompleted image/data[15].

1.2 Motivation

1. The incremental growth in the technology to be anywhere, anytime results in increasing demand for automation in e-health. The need for automatic diagnosis applications with less time complexity and accuracy is highly preferred.
2. Brain disease prediction and detection is the most critical issue in clinical automation workflow. They need an accurate image analysis preprocessing step for gaining high accuracy. The medical image registration is considered the most convenient preprocessing step that can be applied at the beginning of any diagnosis application.

1.3 Problem Statement

The medical image registration involving combines two or more images from different modalities or from various sensors on the same scene

geometrically to provide accurate and detailed patient information across a variety of medical media during clinical treatment [3]. Concisely, MIR requires finding the optimal transformation producing the best fitting between typically two images and the degree of resemblance between them ranked by a similarity metric. Such a transformation calculation expresses as an optimization problem. Optimization problem is solved by an iterative procedure to properly explore the search space of hopeful solutions to the problem.

The optimization process is affected by image noise, image discretization, and orders of magnitude, giving incorrect registration transformation in the case of classical Iterative Closest Point (ICP) algorithm estimations since they are likely to be trapped in local minima[6] . Also, providing accurate results in a reasonable time without stuck in a local minima increases algorithm complexity[7]. On the other hand, the risk of brain tumor is very high among all the various types of cancers, so in order to save life, prompt detection and accurate diagnosis are required for proper treatment. The detection of these cells is a difficult problem and aggressive task if it assessed by human. Therefore, the world moved towards the classification, identification and automatic diagnosis of the detection of dormant cancer cells. The need for an automatic classification process with accurate results is a high-demand requirement. In this thesis the following issues are addressed:

1. A robust MIR approach that overcome the local minima and execution time less than 1 minute.
2. An automatic trust classifier that classify the brain tumor (normal/abnormal) in MRI .

1.4 Aim and Objective

This work aims to develop a soft computer model for registration medical images. Through which a complete picture with more details and more useful information is obtained than the original image. Then the integrated image enters the classification system to classify its magnetic resonance images, of brain tumors into normal and abnormal, and then send the diagnostic result to the patient directly via the mobile . All of these processes are automated. This work has the following objectives:

1. Design and build a hybrid system that includes two main components medical image registration model and classification model.
2. To develop a MIR model that combine the match based with parameter based approach. Using GA as optimizer and (wavelet transform and fusion) as a match based method and transformation to produce more accurate results.
3. To develop a fuzzy –PNN classifier model for proving the accuracy of the MIR stage and automate the classification procedure.

4. To develop a transmission model (Arduino and GSM) based on the cellular network that enables diagnosis automation in the clinical.

1.5 Contribution

The following contributions are conducted from the proposed work,

1. Propose and develop a model for a MIR approach based on Haar wavelet and fusion techniques (maximum, average) with the GA. The entropy of the proposed approach output is higher than the approach with only wavelet or fusion.
2. Develop an accurate fuzzy- PNN classifier model. By Approximation, the features extracted from the images to a fuzzy model, then input into PNN to classify the images and make the final decision.
3. Develop an accurate automatic system for brain tumor classification in MRI images by entering the image into the IR stage for the purpose of analysis and extracting powerful features, then heading to the classification stage using fuzzy-PNN classifier model when assessed incomplete image details, which result in misclassification when conducted by a human.

1.6 Related Works

This section views the previously established works from two viewpoints, the first studies in medical image registration. The second examines the works on classification or diagnosis in the medical Image. To date, several studies have investigated medical image registration field. In context several studies have begun to examine wavelet-based image registration using it for similarity measurements, transformation techniques and/or resampling methods other studies examines the fusion mechanism for the same purpose in this lecture these studies have been examined focusing on their finding in this field:

- In [16]. Been suggested an algorithm for “image registration” based on a wavelet, where they are used to extract features and correspondence rather than the use of intensity values. The preliminary results have demonstrated that the algorithm has a 36,6824 PSNR, and 3,7361 RMSE, this shows a potentially high-performance registered image algorithm. However, a lot of work is required deciding about how the algorithm works; for example, the algorithm is not fast enough, the algorithm robustness has not yet been established, and multi-modal registration has not yet been checked.
- In [17]. For multimodal “image registration”, where mutual Information can be used. However, this approach has limitations, that

remain unsolved. Fusion can handle images of various spectral and spatial resolutions based on a wavelet. This approach cannot however handle situations in which data are spread or input pictures differ considerably in their spectral or spatial resolution.

- A new registration method for medical images based on simplified multiwavelet transform in [18] , based on the combination of special and frequency image information, is proposed. The approach is to register roughly and to register fine. The contour lines of the pair of images are resampled in the rough registration process and are recorded by the Principal Axis system. The pair images are decomposed by the simplified multi-wavelet transform with the fine registration process. The high-frequency coefficients to be reported are also filtered by the high-frequency sub band threshold, which is the mathematical assumption. In the fine registration process, the hierarchical registration technique is applied. Experiments have shown that the approach proposed can produce accurate results for registration. However, there is no evidence or reference to support the assessment findings.

- This paper[19]. suggests a technique to fusion types of MRI images, such as T1 (T1w), T2 (T2w). “MRI” scanning technique is widely used, especially to detect brain and stroke all forms. In order to fuse different types of MRI images of equivalent patients to enhance the diagnosis of their brain diseases, a gradient-based discrete wavelet transformation is

proposed. The first step involves the decomposition of the DWT for fusing picture 1. The second stage consists of gradient calculation of the fused image 1 for the final fused image to be clearly visible for the detection of anomalies. There have been many image fusion techniques, but the output few of them analysis is considered. The approach involves discrete wavelet transformation (DWT), principal component analysis (PCA) and dual-tree complex wavelet transform (DTCWT).

The results included fusion symmetry, standard deviation, reciprocal detail, mean gradient and entropy. Results of experiments indicate that T2W is stronger than other fusion results such as T1w and T2w, T1w for tumor classification using the proposed process. Since the suggested approach gives (90%) precision in comparison to all other methods despite all the possible combinations.

In the context of medical image diagnosis, a considerable amount of literature has been published on automatic detection. These studies are:

- In this work [20], Brain tumors have been classified into three types: Normal, Benign, and Malignant using PNN. First, Feature has extracted by using the Gray Level Co-Occurrence Matrix (GLCM). Then, Image recognition and image compression were done by using the Principal Component Analysis (PCA) method. The author concludes that PNN is

the fastest learning algorithm with high speed and provides accurate results. However, this conclusion is not supported by the actual computational results that demonstrate the accuracy of the PNN and its speed.

- In this work [21], automatic brain tumor classification is proposed by using Convolutional Neural Networks (CNN) classification. The deeper architecture design is performed by using small kernels. The weight of the neuron is given as small. Experimental results show that the CNN archives rate of 97.5% accuracy with low complexity and compared with the all other state of arts methods Benchmark (BRATS) 2015 testing dataset, Image net database is used for classification. It is one of the pre-trained models. So the training is performed for only final layer. the Gradient decent based loss function is applied to achieve high accuracy. The training accuracy, validation accuracy and validation loss are calculated. The training accuracy is 97.5%. Similarly, the validation accuracy is high and validation loss is very low.

- The author in [22] used a DL architectures for classifying a dataset of 66 brain MRIs into 4 classes e.g. normal, glioblastoma, sarcoma and metastatic bronchogenic carcinoma tumors. The classifier was combined with the discrete wavelet transform (DWT) the powerful feature extraction tool and principal components analysis (PCA) and the

evaluation of the performance was quite good over all the performance measures.

- The author in [23] develop a free web-based software based on deep learning that can be utilized in the diagnosis and detection of brain tumors (Glioma/Meningioma/Pituitary) on T1-weighted magnetic resonance imaging. The Keras library, which is used in Python programming language, is utilized in the construction of the deep learning algorithm in this software. The experimental results show that this software can be used for the detection and diagnosis of three types of brain tumors. This developed web-based software can be publicly available at <http://biostatapps.inonu.edu.tr/BTSY/> in both English and Turkish.

- In this work [24] The most common brain tumors, glioma, meningioma and pituitary, are classified using convolutional neural networks. The convolutional network is trained and tested on an accessible Figshare dataset containing 3064 MR images using four different optimizers. AUC, sensitivity, specificity and accuracy are used as performance measure. The proposed method is comparable to the literature and classifies brain tumors with an average accuracy of 96.84% and a maximum accuracy of 97.75%.

- This[25] method is supposed to both prone to human errors and causes excessive time consumption. In this study, the most common brain tumor types; Glioma, Meningioma and Pituitary are classified using deep learning models . classification system with an accuracy up to 90%.

Table (1.1) List of Related Works(IR)

Source	Work content	Model type and Image	The technique used	Results	Notes
[16]	Proposed algorithm for Image Registration to extract features and correspondence instead of using density values.	LAIR data of the CLIF2007 data set provided by Wright-Patterson Air Force Base.	Based on wavelet	The algorithm has a 36,6824 PSNR, and 3,7361 RMSE, a potentially high-performance registered image algorithm.	The algorithm is not powerful, not very fast, and has not been applied to every data set
[17]	Multimodal “image registration”, using mutual Information .	series of images using digital camera on a leveled tripod in front of	Fusion ,wavelet and mutual Information	wavelet harmonic approach and the mutual information gives better	when time is an important constraint one cannot use this method.

		Hiranandani complex, Kharghar, Navi Mumbai		results It can deal with images of different spectral and spatial resolutions. When time is an important constraint one cannot use this method.	
[18]	A new registration method for medical images .The approach is to register roughly and to register fine.	CT images, MR images	simplified multiwavelet transform	The approach proposed can produce accurate results for registration. There is no evidence or reference to support the assessment findings.	There is no evidence or reference to support the assessment findings.
[19]	Suggesting a	MRI images	(DWT),	Results of	The proposed

	technique to detect strokes of all kinds.		(PCA) (DTCWT).	experiments indicate that T2W is stronger than other fusion results such as T1w and T2w, T1w for tumor classification . Since the suggested approach gives (90%) precision in comparison to all other methods	approach was not verified by Apply it to a multimodal image registration.
--	---	--	----------------	---	---

Table (1.1) List of Related Works(Automatic Detection)

Source	Work content	Model type and Image	The technique used	Results	Notes
[20]	Brain tumors have	Brain MRI	PNN,(GLC	PNN is the fattest	This approach is

	been classified into three types: Normal, Benign, and Malignant using PNN.	scans	M), (PCA)	learning algorithm with high speed and provides accurate results.	not supported by the actual computational results that demonstrate the accuracy of the PNN and its speed.
[21]	automatic brain tumor classification is proposed by using Convolutional Neural Networks (CNN) classification.	Brain MRI scans	CNN	The CNN archives rate of 97.5% accuracy with low complexity.	The complexity is low. But the computation time is high.
[22]	Used DL architectures Classification of brain tumors into 4 classes . normal, glioblastoma, sarcoma and metastatic bronchogenic	Brain MRI scans	(DWT), (PCA)	using the DNN classifier shows high accuracy compared to traditional classifiers.	The approach takes time to process in addition to that Images are large (256 x 256).

	carcinoma tumors.				
[23]	Developed a free, web-based program based on deep learning to diagnose and detect brain tumors. The most common brain tumors are glioma, meningioma and pituitary gland	Brain MRI scans	CNN	performance metrics are higher than 98% for classifying the types of brain tumors on the training dataset.	selecting and creating these algorithms may require a lot of time and experience.
[24]	The most common brain tumors, glioma, meningioma and pituitary, are classified	Figshare dataset containing 3064 MR images	CNN	The proposed method is classified brain tumors with an average accuracy of 96.84% and a maximum accuracy of 97.75%.	It can take a lot of time and get a little complicated.
[25]	the most common brain tumor types; Glioma, Meningioma and	Brain MRI scans	deep learning models	The system which has been built has an accuracy of up to	This method is supposed to both prone to human errors and

	Pituitary are classified		90%.	causes excessive time consumption.
--	-----------------------------	--	------	--

1.7 Thesis organization

This thesis consists five chapters including the present one:

- **Chapter Two :Theoretical Background:** Includes the chapter the theoretical background of the concepts, tools, and techniques that were used in the design and implementation of the proposed (Introduction system , soft computing , medical image and Transmission model) .
- **Chapter Three: A Soft Computing Model For Image Registration And Classification:** This chapter includes the designing details the proposed model for a soft computing model for medical image registration in internet of thing environment with the general diagram of the system and a detailed explanation of the tools and algorithms that were used in the system.
- **Chapter Four: Implementation Result And Discussion:** It includes reviewing the results obtained from the implementation of the proposed

system, as well as discussing and analyzing these results, and then making comparisons with previous research and studies.

- **Chapter Five :Conclusion and Suggestions for Future Work:** This chapter includes the most important conclusions that were obtained in addition to the future work recommended by the research.

CHAPTER TWO

THEORETICAL BACKGROUND

2.1 Introduction

This chapter includes the theoretical background of the concepts and algorithms that are included in this model where it was discussed (a soft computing model , medical image registration , internet of thing).

2.2 Image Registration

Image registration, also known as image fusion, matching or warping, can be defined as the process of aligning two or more images. Image registration is a crucial step for image analysis in which valuable information is conveyed in more than one image; i.e., images acquired at different times, from distinct viewpoints or by different sensors can be complementary. Therefore, accurate integration (or fusion) of the useful information from two or more images is very important[26].

2.3 Image Registration Approach

Image Registration approach is divided into matching-based and parameter-based. Both are explained with brief details below.

a- The matching-based approach works by looking for a set of correspondences of pairs of similar image features. Then, the registration transformation is derived from that set.

The main drawback is its sensitiveness to the initial transformation getting stuck in local optima[6]. This approach elaborated in the following steps[7]:

1. Preprocessing: modifies both the sensed (input) and reference (base) image to improve the performance of the feature selection and feature correspondence of image registration because some images may be blurry or have a significant amount of noise which will dramatically affect the outcome of the algorithm. Some techniques alleviating the noise (Image Smoothing) are median filters, mean filters, Gaussian filters. Also, the techniques for deblurring (Image Sharpening) are the Laplacian, high boost filtering, gradient.
2. Feature Extraction: selects the key features such as corners, lines, edges, contours, templates, regions. Which will be used to do feature correspondence. Some examples of feature selection are Harris corner detector, gradient, Hough transform.
3. Feature Correspondence: matches the key features selected in the reference image and the sensed image to see which points in the reference image match with the points in the sensed image. Cross-correlation, mutual information, template matching, Chamfer are a few examples of feature correspondence.

4. Transformation Function aligns the sensed image to the reference image by the mapping function. A few examples of transformation functions are affine, projective, piecewise linear, thin-plate spline.

b. The parameter-based IR approach directly explores the values in the range of each transformation parameter and is summarized as below [27], and shown in Figure (2.1).

1. Two input Images named scene I_s and model I_m .
2. A Registration transformation f , relating the two images. Typically, it is a parametric function.
3. A Similarity metric function F . It aims to measure a qualitative value of closeness or degree of fitting between the transformed scene image, noted by $f(I_s)$, and the model image.
4. An Optimizer. It is a method that seeks the optimal transformation f inside the defined solution search space.

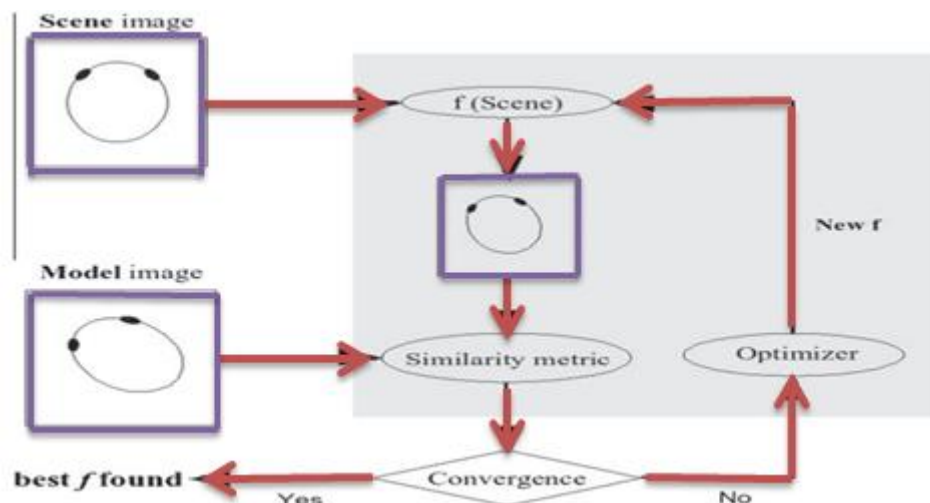


Figure (2.1) Image Registration [27]

2.3.1 Medical Image

It is a process and technique that create a visual impersonation of the interior of a body for medical intervention and clinical analysis, as well as visual representation of the functions of some tissues or organs (physiology). Medical imaging attempts to discover the internal structures covered by the skin and bones, in addition to diagnose diseases and treat them. Also, medical imaging establishes a database of normal anatomy and physiology to enable the identification of abnormalities. The most common types of medical imaging:[28].

1- Computerized Tomography (CT Scanners): A computerized tomography scan, more commonly called a CT scan. It uses computers and x-rays to generate a detailed image for the inside of them body. CT scan can present a visualization for blood vessels, bones and internal organs. As well, upper body, such as the brain, neck, spine, chest, and sinuses are commonly scanned. The picture of a CT scanner as shown in Figure (2.2). They are frequently used in diagnosis, for example to find tumors, or to see broken bones[29].



Figure (2.2) Picture of a CT Scanner[29]

2- Magnetic Resonance Imaging (MRI Scanners): (MRI) is a non-invasive biomedical imaging technique that make use of a powerful oscillating magnetic field to induce endogenous atoms such as hydrogen, or exogenously added contrast agents, to emit radio waves that are detected and used to create images (2D and 3D) of a living subject in the MRI scanner. Unlike conventional x-rays, there is no exposure to ionizing radiation and at most field strengths the procedure is considered safe for nearly every age group. Because it is non-invasive and possesses excellent spatial resolution, over the past decade the use of MRI as a research tool has exponentially increased [30].

The range of MRI uses has started from add-ons to clinical study to the studies brain studies in developing children. furthermore, the recent years have witnessed efforts to use MRI in studying the function of brain. The traditional patient diagnosis and treatment in medicine have been changed once and for all by the emergence of MRI and functional magnetic resonance imaging (fMRI) of the brain. Rather than employing invasive procedures at the current time physicians can literally view the internal body structures and understand and map the function of brain related to behaviors, feelings, and task clearly. MRI scans were used in this study[31]. The MRI scan as shown in Figure(2.3).

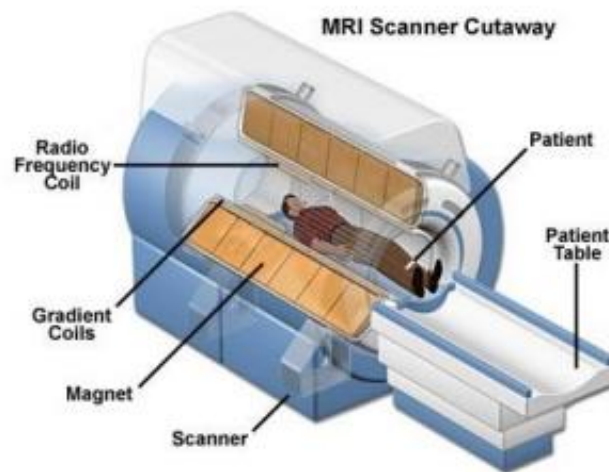


Figure (2.3) MRI Scan[31]

3- PET Scanner: Positron emission tomography (PET): This scanner is able to create 3D images to the internal organs. These images are merged with MRI and CT scans to generate a more accurate image for detailed reading. It is also possible to focus them on a certain part of the body, and show how well the work of the body is[32]. The form in which the CT and PET scans are combined is shown in Figure (2.4).

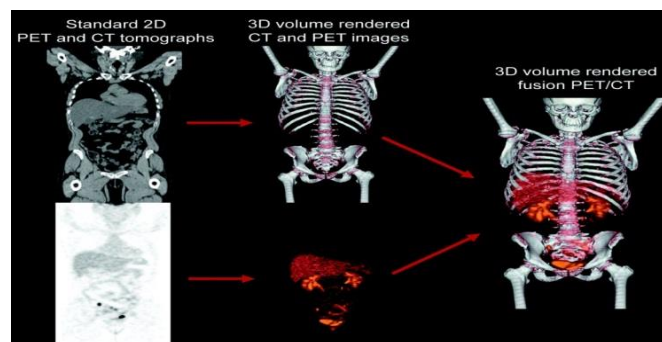


Figure (2.4) Combination of a CT Scan and a PET Scan[33]

They are used at planning surgeries like heart or brain operations. Also, this technique is usually used with those who have been diagnosed with cancer to know the extent to which the cancer has spread or its response to treatments as chemotherapy[33].

4- Ultrasound: It uses sound waves with high frequency broadband that are reflected by the tissues to different degrees and produce images (2D and 3D). Although its output images give less detailed images than MRI and CT, it is ideal in many situations, in particular at studying the function of moving structures in real-time, emits no ionizing radiation. An ultrasound image as shown in Figure (2.5). Usually ultrasound is used to image the fetus in women's uterus. However, the uses of ultrasound technique are much wider, including imaging the abdominal organs, breast, tendons, veins, heart, muscles and arteries[34].



Figure (2.5) An Ultrasounds [34]

5- X-Rays: They use the x-ray part of radiation of the electromagnetic spectrum. The most frequent use of x-ray is to obtain images of inside of the body[35]. Also they can create images to diagnose if a bone is broken and bones tumors, where x-rays guide surgeons during an operation. Dentists also use x-rays to view the teeth[35]. The diagram of how an x-ray scanner works is shown in Figure (2.6).

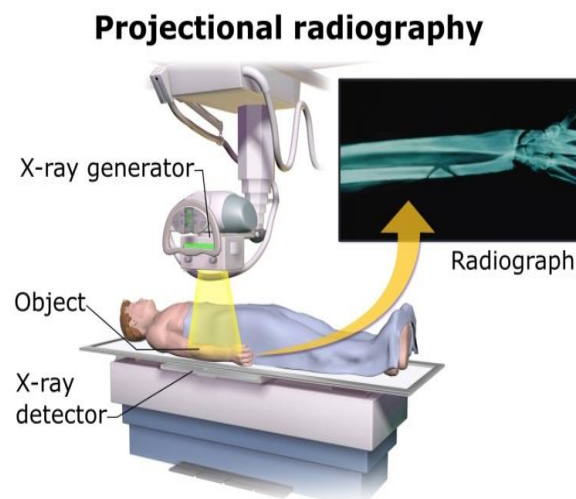


Figure (2.6) Diagram of How an x-ray Scanner Works[35]

2.3.2 Feature Extraction

During the process, characteristic features and objects (such as the significant regions, edges, angles, dots or lines, etc.) are extracted from the frames and sensed images. The gravity control center (CPs), line ends, markers points, object contours, coastal lines, roads, line crossings and road crossings, which are invariant in the spirit of rotation , scaling,

translation and skewing, are expressed in these characteristics[36].

There are many methods and algorithms used to extract features. Each method or algorithm aims to extract a specific type or special part of the features in the images, some of which may be complementary to some of them[37]. These types were used in the proposed system:

2.3.2.1 Local Binary Patterns (LBP)

It is a type of visual descriptors utilized for classification in computer vision. It has been identified as a strong feature for texture classification. Furthermore, it was found out that when LBP is combined with histogram of oriented gradients (HOG) descriptor, it considerably enhances the detection performance on several datasets[38].

The simplest version of LBP operator sets the value of center pixel as a threshold to (3*3) neighbor pixels. Thresholding will generate a binary pattern that represents texture characteristic. Following is the equation of basic LBP[39]

$$LBP(X_c, Y_c) = \sum_{n=0}^8 2^n g(I_n - I(X_c, Y_c)) \quad (2,1)$$

Where

LBP (xc, yc): is a LBP value at the center pixel(xc, yc).

$I(xc, yc)$: are the values of neighbor pixel and center pixel respectively.
 n : is the index of neighbor pixels.

2.3.2.2 Speeded up Robust Feature (SURF)

Is a scale and rotation invariant interest point detector and descriptor. Compared to the earlier proposed methods, it approximates or outperforms them in terms of distinctiveness, repeatability, and it can be compared and computed much faster. The work of "SURF" feature detector relies on second order Hessian matrix. It uses the box filter and integral images to accelerate the computation. The integral image is a cumulative image in which a single point $p(x,y)$ corresponds to the summed values of all points above and to the left of $p(x,y)$ [40].

Hessian matrix $H(x, \sigma)$ for a point X at scale (σ) is defined as follows[39]:

$$H(x, \sigma) = \begin{bmatrix} L_{xx}(x, \sigma) & L_{xy}(x, \sigma) \\ L_{xy}(x, \sigma) & L_{yy}(x, \sigma) \end{bmatrix} \quad (2.2)$$

Where, $L_{xx}(x, \sigma)$ is the convolution of the Gaussian second order derivative with the image at point X .

The computation speed is increased when employing the uses of "SURF" as an approximation of the 'Gaussian second order' partial derivatives.

This yields the determinant of the updated hessian matrix as given in Equation (2.3).

$$\text{Det(Happox)} = D_{xx}D_{yy} - (0.9D_{xy})^2 \quad (2.3)$$

Where,

D_{xx} , D_{xy} and D_{yy} are the approximation of L_{xx} , L_{xy} and L_{yy} .

2.3.2.3 Binary Robust Invariant Scalable Keypoints (BRISK)

This algorithm performs key point detection, description & matching as follows: It uses the same method, as FAST, for computing all key-points in images and in scale space. But only (9-16) mask is used, this means that: 9 of 16 pixels should be either darker or brighter (minima or maxima) to the center pixel (threshold satisfying pixel). It applies 9-16 detectors on all octaves & intra-octaves to figure out all regions of interest then subjected them into non-maximal suppression to find actual interest points[41].

It performs point to point comparison of intensity to reach key-points description. This descriptor is made of binary string. It compiles the results of simple brightness comparison test and forms the binary string. It sets bit 1 when intensity of first pixel is higher than second & 0 otherwise.

It computes the local gradients (magnitude, orientation) across each interest point for orientation & rotation invariance. It creates short pairs

(those with distances below threshold) and long pairs (those with distances above threshold). The short pairs are used for intensity comparison that build the descriptor while long pairs are used for orientation determination [41].

In order to avoid aliasing effects when sampling the image intensity of a point p_i in the pattern, was applied Gaussian smoothing with standard deviation σ_i proportional to the distance between the points on the respective circle. Positioning and scaling the pattern accordingly for a particular keypoint k in the image, [39] one of the $N \cdot (N - 1)/2$ sampling-point pairs (p_i, p_j) . The smoothed intensity values at these points which are $I(p_i, \sigma_i)$ and $I(p_j, \sigma_j)$ respectively, are used to estimate the local gradient $g(p_i, p_j)$ by [39].

$$g(p_i, p_j) = (p_j - p_i) \cdot \frac{I(p_j, \sigma_j) - I(p_i, \sigma_i)}{\|p_j - p_i\|^2} \quad (2.4)$$

Where

$g(p_i, p_j)$ the local gradient

$I(p_i, \sigma_i)$ and $I(p_j, \sigma_j)$ intensity values

σ standard deviation

p_i the point in the pattern

2.3.2.4 Harris Detector

Computer vision algorithms frequently use this operator in the extraction of image features and corners. Harris's corner detector has shown more accuracy at differentiating between edges and corners. Instead of using shifting patches for each 45-degree angles, this detector regards the differential of the corner score with directly referencing to the direction. This detector has been enhanced, and many algorithms adopted it for application of image preprocessing .

Corners represent an essential part of images, where generally they can be termed as interest points that are not affected by illumination, translation, and rotation [42]. Been seen that corners are regions in the image with large variation in intensity in all the directions. From this simple idea, a mathematical form was obtained by Harris. Essentially, the difference intensity for a displacement of (u,v) is to be found in all directions, which can be expressed as follows[39]:

$$E(u,v) = \sum w(x,y) [I(x+u, y+v) - I(x,y)]^2 \quad (2.5)$$

The window function is either a rectangular window or a Gaussian window which gives weights to pixels underneath. This was maximized this function $E(u,v)$ for corner detection. That means Must be maximize the second term. The final equation is generated through several mathematical steps and applying Taylor expansion to the result is as follows[39]:

$$E(u, v) \approx [u \ v] M \begin{bmatrix} u \\ v \end{bmatrix} \quad (2.6)$$

Where

$$M = \sum w(x,y) \begin{bmatrix} I_x^2 & I_x I_y \\ I_x I_y & I_y^2 \end{bmatrix} \quad (2.7)$$

Here, the derivatives of an image in x and y directions are I_x and I_y respectively. Then comes the main part. After this, they created a score, basically an equation, which determines if a window can contain a corner or not[39].

$$R = \det M - K(\text{trace } M)^2 \quad (2.8)$$

Where

$$\det M = \lambda_1 \lambda_2$$

$$\text{trace } M = \lambda_1 + \lambda_2$$

Harris corner detector as shown in Figure(2.7). λ_1 and λ_2 are the eigenvalues of M . So the magnitudes of these eigenvalues decide whether a region is a corner, an edge, or flat. When $|R|$ is small, which happens when λ_1 and λ_2 are small, the region is flat. When $R < 0$, which happens when $\lambda_1 \gg \lambda_2$ or vice versa, the region is edge. When R is large, which happens when λ_1 and λ_2 are large and $\lambda_1 \sim \lambda_2$, the region is a corner[43].

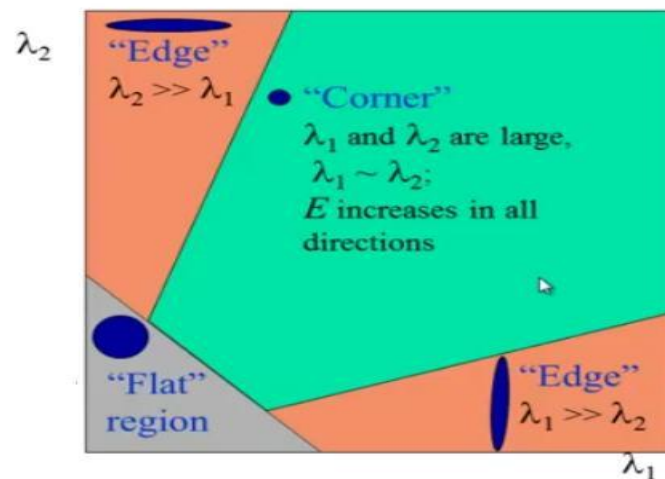


Figure (2.7) Harris Corner Detector[43]

2.3.2.5 Minimum Eigenvalue Algorithm (Min Eigen)

In a minimum of value of an independent corner detection, a measurement of the difference in intensity due to local integration window changes in both directions is determined by determining the corner reaction of each pixel. The MinEigen measures its own value directly and selects the points whose minimum value exceeds the specified threshold. The detector MinEigen is easy to measure and insensitive to variation of the image[44].

The function of this algorithm is slightly different than that of Harris. The latter uses corner selection criteria with the help of Response function (R). If a certain value is less than (R), then the point will be

called ‘corner’, where the score function is computed by the use of two eigen values as Figure (2.8) shows.

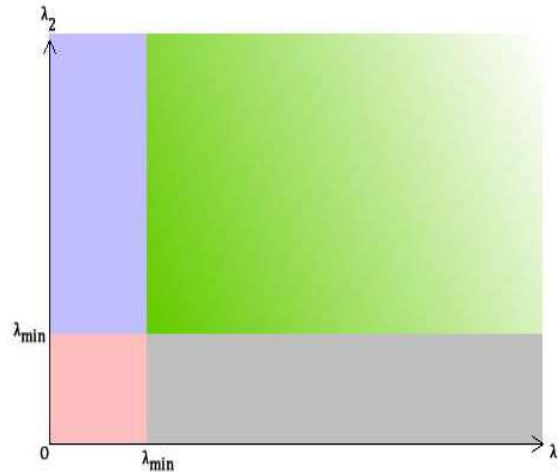


Figure (2.8) Min Eigen[44]

$$R = \min(\lambda_1, \lambda_2) \quad (2.9)$$

Pink and gray blue regions indicate that the value is less than required minimum, so they can be edge or flat regions. While green region indicate that the values are more or above the required certain value. Hence, the pixels in this region can be named as corners [44]. Figure(2.9) showing the use of these algorithms to extract features.

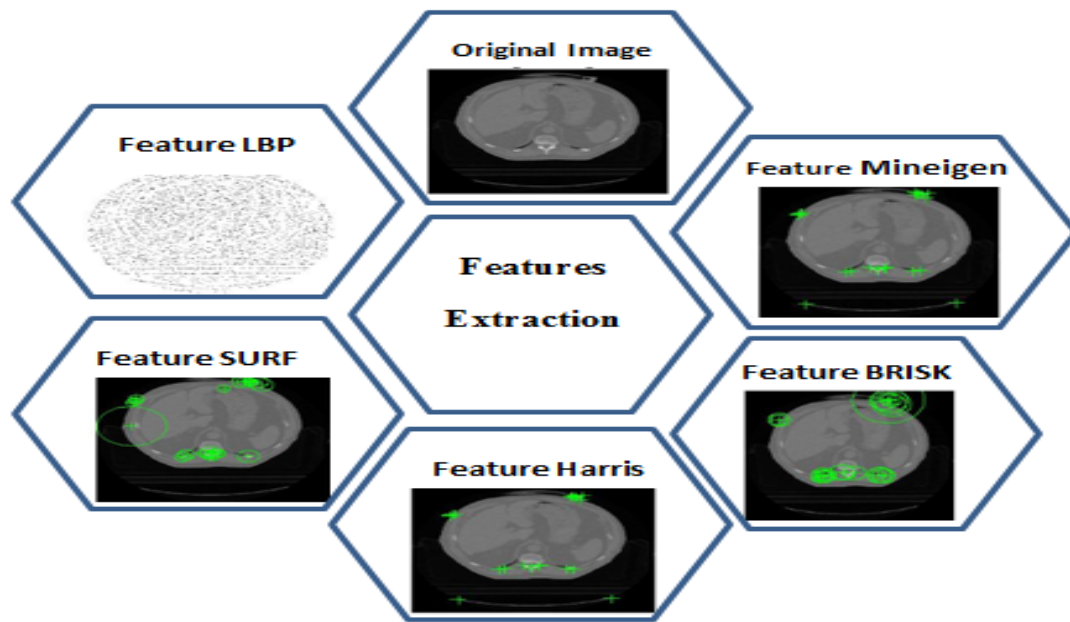


Figure (2.9) The Feature Extraction Stage

2.4 Image Enhancement

The image improvement stage is one of the most important treatment steps in a treatment field digital photos. Image optimization techniques are used by removing noise or adjusting colors or adjust the illumination intensity.

The image may be damaged due to random differences in and differences in illumination or poor contrast that has to be density dealt with in the early stages of vision processing. Therefore filters that aim to eliminate these undesirable properties are used. There are several types of filters, each with specific features[45].

One of the most frequently used filters is it Gaussian filter. It was used in the image enhancement process in this study. In image processing, a Gaussian blur (also known as Gaussian smoothing) is the result of blurring an image by a Gaussian function[46] . In two dimensions, it is the product of two such Gaussian functions, one in each dimension[39]:

$$\mathbf{Gaussian\ Kernel\ 2D} = \frac{1}{2\pi\sigma^2} e^{-\frac{(x^2+y^2)}{2\sigma^2}} \quad (2.10)$$

Where

x is the distance from the origin in the horizontal axis

y is the distance from the origin in the vertical axis

σ is the standard deviation of the Gaussian distribution.

This results in a blur that preserves boundaries and edges better than other, more uniform blurring filters.

2.5 Image Fusion

The image fusion process is defined as gathering all the important information from multiple images, and their inclusion into fewer images, usually a single one. This single image is more informative and accurate than any single source image, and it consists of all the necessary information. The purpose of image fusion is not only to reduce the

amount of data but also to construct images that are more appropriate and understandable for the human and machine perception[47].

Various techniques of image fusion can be classified as pixel level, decision level and feature level. Pixel level techniques for image fusion directly integrate the Information from input images for further computer processing tasks. Feature level techniques for image fusion entails the extractions of relevant features that is pixel intensities, textures or edges that are compounded to create supplementary merged features. In decision level fusion techniques for images, the input images are processed one at a time for the extraction of Information [48]. The Figure(2.10) shows the fusion stages of the images.

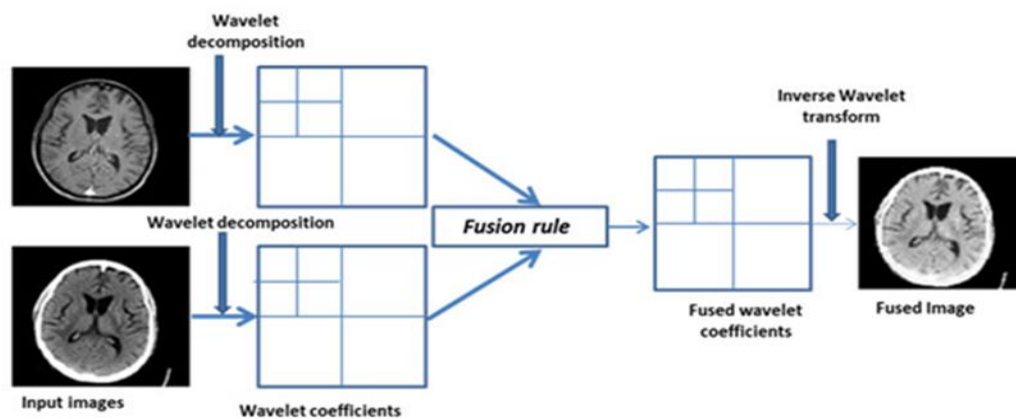


Figure (2.10) The Fusion Image Stage[48]

Due to recent technological developments, different image fusion techniques. They have been used in many applications including video surveillance, security, remote sensing, machine vision, and medical Photography[49].

Image Fusion Methods: In order to better demonstrate that existing image fusion methods can be accommodated by the framework of the GIF method, the mathematical models of a number of methods are sorted into one group of typical exemplars rather than investigating all of the existing methods exhaustively[50].

1- IHS Transform: The IHS technique is a standard procedure in image fusion, with the major limitation that only three bands are involved. Originally, it was based on the RGB true color space. It offers the advantage that the separate channels outline certain color properties, namely intensity (I), hue (H), and saturation (S). The IHS technique usually comprises four steps: 1) transform the red, green, and blue (RGB) channels (corresponding to three multispectral bands) to IHS components; 2) match the histogram of the panchromatic image with the intensity component; 3) replace the intensity component with the stretched panchromatic image; and 4) inverse-transform IHS channels to RGB channels. The resultant color composite will then have a higher spatial resolution in terms of topographic texture information.

2- Brovey Transform: The BT is based on the chromaticity transform. It is a simple method for combining data from different sensors, with the limitation that only three bands are involved. Its purpose is to normalize the three multispectral bands used for RGB display and to multiply the result by any other desired data to add the intensity or brightness component to the image.

3-High-Pass Filtering: The principle of HPF is to add the high-frequency information from the HRPI to the LRMI to get the HRMI.

The high-frequency information is computed by filtering the HRPI with a high-pass filter or taking the original HRPI and subtracting the LRPI, which is the low-pass filtered HRPI. This method preserves a high percentage of the spectral characteristics, since the spatial information is associated with the high-frequency information of the HRMIs, which is from the HRPI, and the spectral information is associated with the low-frequency information of the HRMIs, which is from the LRMI.

4- Principal component analysis (PCA): The PCA method is similar to the IHS method, with the main advantage that an arbitrary number of bands can be used. The input LRMI are first transformed into the same number of uncorrelated principal components. The first principal component image contains the information that is common to all the bands used as input to PCA, while the spectral information that is unique to any of the bands is mapped to the other components. Then, similar to the IHS method, the first principal component (PC1) is replaced by the HRPI, which is first stretched to have the same mean and variance as PC1. As a last step, the HRMI are determined by performing the inverse PCA transform.

5- Weighted pixel averaging: Weighted pixel averaging approach under the spatial domain of the image fusion is the simplest method in this prospect. The basic advantage offered by this approach is that it has the potential to lessen or decrease the present noise or artifacts within the source of image .It was used in the proposed system.

6- Wavelet Transform method The discrete sampling of wavelets is the basic function performed by the DWT. The advantage offered by this approach is its tendency to favor of handle the temporal resolution . Another significant advantage offered by DWT is that holds information of location together with the details of frequency factor. The domain comprised of applications of DWT is massive enough that it encompasses areas including mathematics, engineering, robotics science and computer science. Another major solicitation of DWT is in the domain of signal processing. It was used in the proposed system.

2.5.1 Discrete Wavelet Transform

DWT method decomposes the two or more images into various high and low-frequency bands. This method minimized the spectral distortion in the resultant fused images by producing the good signal to noise ratio.

wavelet is considered a powerful image processing technique. It includes matchless information at the various resolution, it is able to generate directional bands (low-low, low-high, high-low and high-high) and it is more compact. Image fusion based on other methods performs less when compared to those based on wavelet transform. The DWT show in Figure (2.11).

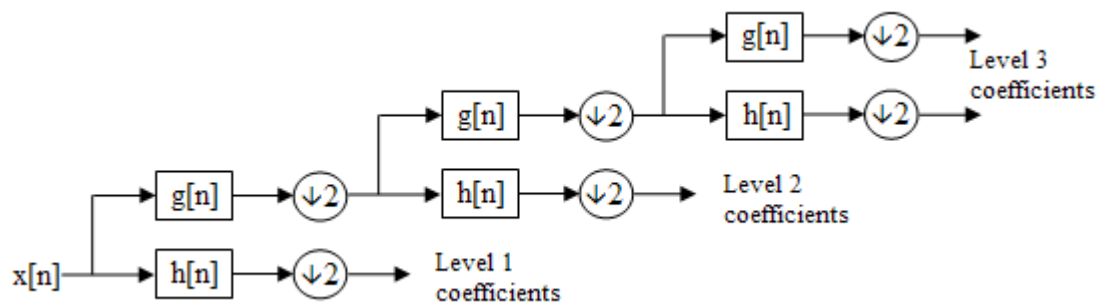


Figure (2.11) Discrete Wavelet Transform [51]

Image processing is an emerging research area that seeks attention in the biomedical field. There are lots of image processing techniques that are not only useful in extracting useful information for analysis purpose but also saves. computation time and memory space. The two-dimensional Discrete Wavelet Transform (DWT) has shown considerable promise in image processing applications, such as the JPEG2000 still image compression standard and image denoising. A hardware DWT core could be integrated into a digital camera or scanner to perform image processing inside the device. Research on DWT architectures and hardware implementations includes efficient filter/subsample-based architectures as well as implementations based on the lifting scheme[51]. The DWT in image processing show in Figure(2.12).

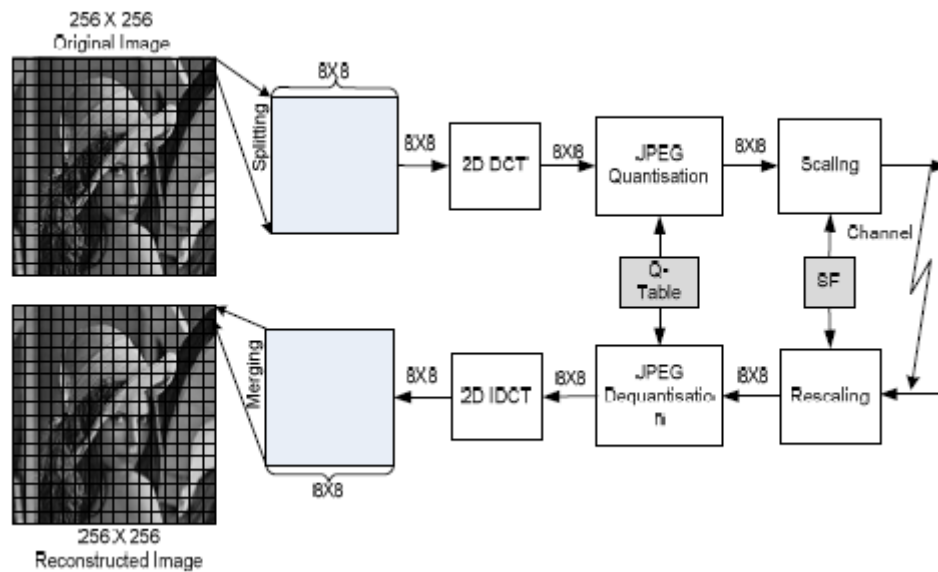


Figure (2.12) DWT in Image Processing [51]

It is able to detect local features in signal processing. Also, it can be used to decompose signal with dimensions, as two-dimensional gray-scale image signals, into different resolution levels for multiresolution analysis. The Main type of DWT is:

1- Haar wavelets: the Haar wavelet is a sequence of rescaled "square-shaped" functions which together form a wavelet family or basis. Wavelet analysis is similar to Fourier analysis in that it allows a target function over an interval to be represented in terms of an orthonormal basis. The Haar sequence is now recognized as the first known wavelet basis and extensively used as a teaching example. The Haar wavelet is also the simplest possible wavelet. The technical disadvantage of the Haar wavelet is that it is not continuous, and therefore not differentiable. This property can, however, be an advantage for the analysis of signals with

sudden transitions (discrete signals), such as monitoring of tool failure in machines. Haarr wavelet were employed in this study [52].

Use Haar wavelet equation where H is Haar mask :

$$H = \frac{1}{\sqrt{2}} \begin{bmatrix} 1 & 1 \\ 1 & -1 \end{bmatrix} \quad (2.11)$$

$$I(x, y) = \frac{1}{4} \sum_{k_1=1}^2 \sum_{k_2=1}^2 I(x, y) H(k_1, k_2) \quad (2.12)$$

Where

I is the image

K1 is the counter of the row

K2 is the counter of the column

2- Daubechies wavelet: The most commonly used set of discrete wavelet transforms was formulated by the Belgian mathematician Ingrid Daubechies in 1988. This formulation is based on the use of recurrence relations to generate progressively finer discrete samplings of an implicit mother wavelet function; each resolution is twice that of the previous scale. In her seminal paper, Daubechies derives a family of wavelets, the first of which is the Haar wavelet. Interest in this field has exploded since

then, and many variations of Daubechies' original wavelets were developed.

3- The Dual-Tree Complex Wavelet Transform (DCWT):The dual-tree complex wavelet transform is a relatively recent enhancement to the discrete wavelet transform (DWT), with important additional properties. It is nearly shift invariant and directionally selective in two and higher dimensions. The multidimensional (M-D) dual-tree CWT is nonseparable but is based on a computationally efficient, separable filter bank (FB).

2.6 The Entropy

Entropy quantifies the information content of the image. It describes how much uncertainty or randomness there is in an image. The more information the image contains, the better its quality. Entropy is the expected value of the information[53].

The advantage of entropy in image coding context is being the lower limit for the average coding length in bits per pixel which can be reached without losing information through an optimum coding scheme. A number of previous studies have shown that the entropy of images can be utilized to measure the visual aspects of a given image and to collect information and use them as parameters for some systems[54] .

Another widely used interpretation is for measuring the amount of information within an image. Entropy was used in the proposed system to

measure fitness values. The entropy $H(x)$ can be calculated as the following equation states[55]:

$$H(x) = - \sum_{i=1}^n p_i \log_2 p_i \quad (2.13)$$

The p_i value is the occurrence probability of a given symbol. Here, the symbols are the pixels. To simplify it, let's consider a single-channel 8-bit image (256 intensity levels), then can compute p_i value as follows:

$$P_i = \frac{\text{Number of occurrences of the intensity level } i}{\text{Number of the intensity levels}} \quad (2.14)$$

2.7 Soft Computing

Soft computing is a set of practices that intend to utilize tolerance for uncertainty and imprecision to achieve low cost solutions, tractability and robustness. It's basically consisted of neurocomputing, fuzzy logic, and probabilistic reasoning. It is expected that soft computing would contribute significantly to many applications fields as image processing,

e-commerce, software engineering, etc[56].

The core soft computing technology is the fuzzy logic, artificial neural network and genetic algorithm as explained below. The basic soft computing diagram as shown in Figure (2.13).

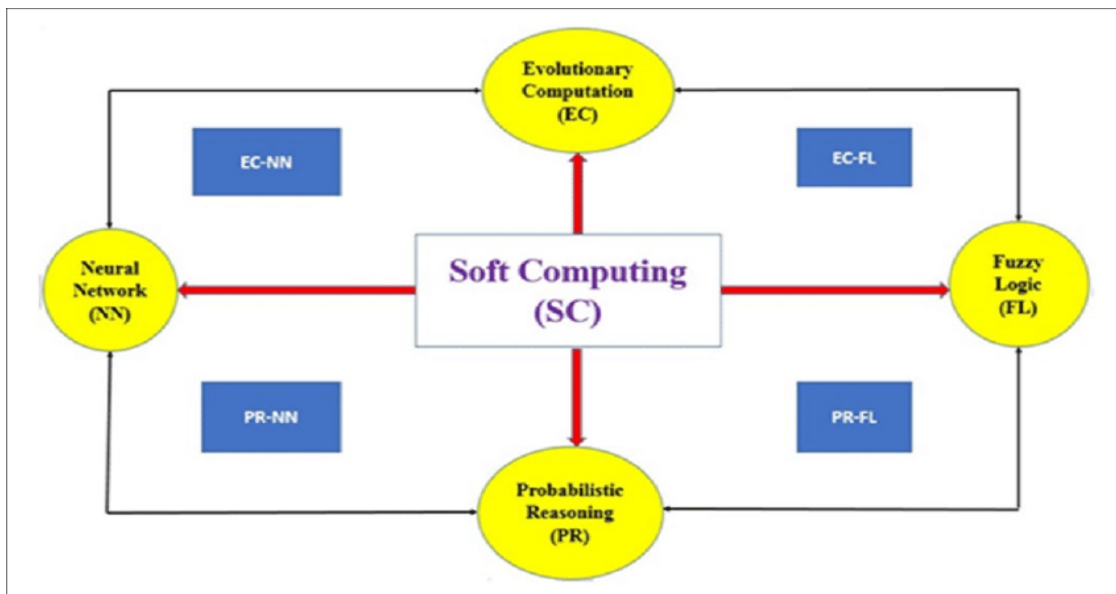


Figure (2.13) Basic Soft Computing Diagram[56]

2.7.1 Fuzzy Logic

Fuzzy logic or 'fuzzy set' is broadly applied in a number of AI (Artificial Intelligence) applications for reasoning due to its ability to distinguish the ambiguity of solutions, and indicating which solution is of degree of ambiguity that is practical to human decisions[57].

'Fuzzy set's' theory acquired its high importance in medical image processing for dealing with accurate data and knowledge. It provides a coherent mathematical structure for information modeling at various levels, knowledge representation, reasoning and decision making and unrelated information fusion.

Imprecision is usually an integral part of images, and several levels can reveal its causes: observed phenomenon (the limits between the objects or the structures are inaccurate), acquisition process (methods of numerical reconstruction, inadequate resolution), and image processing steps (imprecision induced by a filtering for instance). The representation of such imprecisions by fuzzy set's' has a number of advantages [58].

First, they can illustrate different types of imprecision in images, for example, imprecisions in spatial location of objects, or membership of an object to a class. For instance, partial volume effect, which occurs frequently in medical imaging, finds a consistent representation in "fuzzy set" (membership degrees of a voxel to classes or tissues directly represent partial membership to the various tissues mixed up in this voxel, leading to a consistent modeling with respect to reality) [59].

Second, image information can be represented at many levels with "fuzzy sets" (regional, local, or global), as well as under various forms (symbolic, or numerical). For example, very local information is included in the gray-based classification (at pixel level). Regional information is involved at introducing spatial coherence in the classification or relations between features; while for scene interpretation, more global information

is included at introducing relations between objects or regions is related to the field of spatial reasoning. [60].

Third, very different types of information can be represented by the ‘fuzzy set’, which also has the ability to dealing with information derived from exterior knowledge as expert knowledge and data extracted directly from images. This is used in a model-based pattern recognition, in which fuzzy data is brought out from the images, these data are matched and compared to a model that represents knowledge expressed in fuzzy terms [60]. Fuzzy Inference System is shown in Figure (2.14).

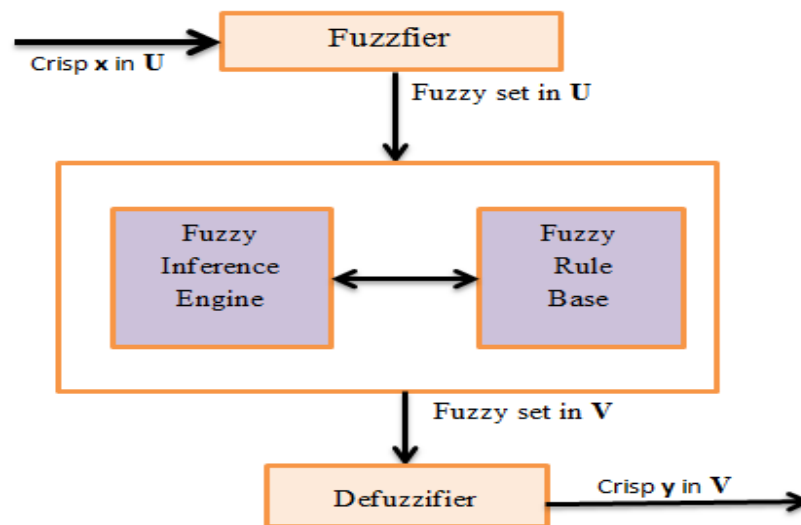
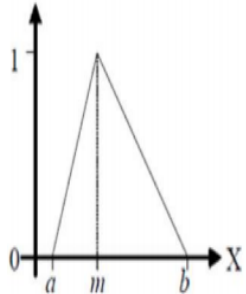


Figure (2.14) Fuzzy Inference System Diagram[60]

To implement fuzzy logic technique in a real application requires the following three steps:

1. Fuzzification : convert classical data or crisp data into fuzzy data or membership functions (MFs)[61]. The type of membership function that was used in the proposed system are shown in the Table (2.1):

Table(2.1) Membership Function

Name of Membership	Mathematical expression	Function shape
<p style="text-align: center;">Triangular</p> <p>It is characterized by low cost, so it is widely used in control applications. They were used in the proposed system</p>	$A(x) = \begin{cases} 0 & \text{if } x \leq a \\ \frac{(x-a)}{(m-a)} & \text{if } x \in (a, m] \\ \frac{(b-x)}{(b-m)} & \text{if } x \in (m, b] \\ 0 & \text{if } x \geq b \end{cases}$	

2. Fuzzy Inference Process: combine membership functions with the control rules to derive the fuzzy output. The ‘IF-THEN’ rule represents the fuzzy rule. It associates a condition described using linguistic variables and ‘fuzzy sets’ to an output or a conclusion. Generally, the ‘IF’ part is utilized to gain knowledge through an elastic condition, while ‘THEN’ is used to generate an output or a conclusion in linguistic variable form. The most common use of this rule is by the fuzzy inference systems for computing the degree to which the input data matches the condition of a rule[62]. The most famous types of fuzzy implication were used in the proposed system shown in the following Table(2.2).

Table(2.2) Types of Fuzzy Implication [62]

Implication	Operator	Also connector
Larsen	$R_L = (\mu X(u) \cdot \mu Y(v))$	Dot
Mamdani	$R_M = \min(\mu X(u), \mu Y(v))$	AND
Zadeh	$R_Z = \max(\min(\mu X(u), \mu Y(v)), 1 - \mu X(u))$	OR, AND
DienesRescher	$R_D = \max(1 - \mu X(u), \mu Y(v))$	OR
Lukasiewicz	$R_k = \min(1, 1 - \mu X(u) + \mu Y(v))$	AND

3. Defuzzification: It is the procedure that generates only one number out of an aggregated ‘fuzzy set’. It is utilized for transferring the results of fuzzy inference into a crisp output. It means that defuzzification realization is made through a decision making algorithm that chooses the best crisp value based on a ‘fuzzy set’ [63]. The type of defuzzification was used in proposed system [64] shown in the following Table(2.3).

Table (2.3) Type of Defuzzification[64]

Methods of Defuzzification	Details of the Method	Formula	NO. Equation
Mean of Maxima Methods	This method considers values with maximum membership. They were used in the proposed system	$D^* = \frac{\sum_{d_i \in N} d_i}{ N }$ <p>$N = \{d_i \mu_A(d_i) \text{ is equal to the height of the fuzzy set } A\}$ and N is the cardinality of the set N.</p>	(2.15)

2.7.2 Neural Network (NN)

Neural Network is inspired by the biological neurons network. It is a network of artificial neurons in which mathematical models, as units of information processing, used to find data patterns that cannot easily be noticed by human [65].

An artificial neural network is a system loosely modeled on the human brain. The field goes by many names, such as connectionism, parallel distributed processing, neuro-computing, natural intelligent systems, machine learning algorithms, and an artificial neural networks. It is an attempt to simulate within specialized hardware or sophisticated software, the multiple layers of simple processing elements called neurons. Each neuron is linked to certain of its neighbors with varying

coefficients of connectivity that represent the strengths of these connections. Learning is accomplished by adjusting these strengths to cause the overall network to output appropriate results. Its important components: inputs, Weights, transfer function, Bias and activation function the most important types (linear, sigmoid, ReLU)[65]. NN includes many types as shown in Figure(2.15) .These types such as[66].

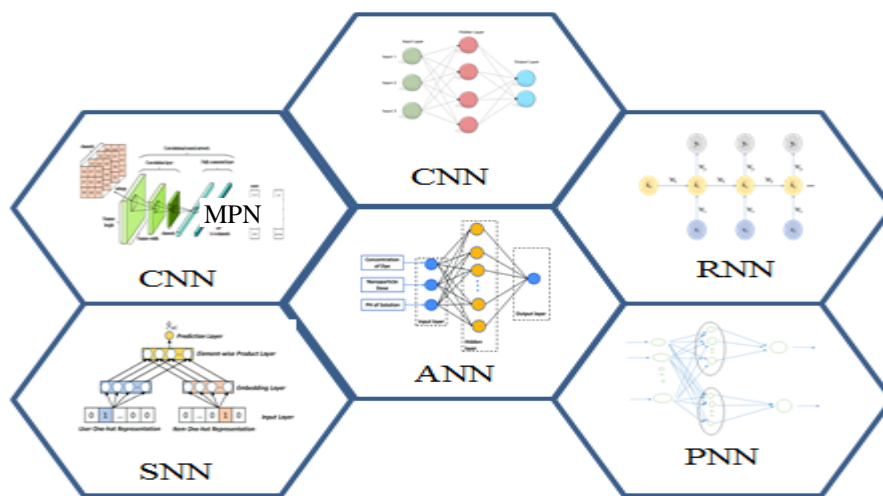


Figure (2.15) The Most Famous Type of Neural Network [66]

2.7.2.1 Details of PNN

A PNN is a neural feed system derived by the Bayesian network and a main fisher discriminant analysis statistical algorithm. It was launched by D.F Specht [67].

Parzen's approach works well in terms of selecting smoothing parameters when the training data gets too large, the approximation

becomes equal to the conditional probabilities of the actual class. In the case where the training data sets are of limited size, the correct selection of smoothing parameters is essential for the good performance of the classifier.

A major problem associated with PNN is how to select the smoothing parameter (s) included in the Gaussian functions used to estimate conditional probabilities. Specht[68] suggested using cross-validation to estimate smoothing coefficients that although simple, faces two major difficulties:

1- Selection the correct candidate values for validation. Although the smoothing parameter represents the standard deviation of a Gaussian nucleus, the smoothing parameter should be chosen less than the standard deviation of the observed cases. The optimum smoothing parameter can be much smaller than the standard deviation of the observed cases. Thus, the theoretical range of the optimum smoothing parameter is infinitely wide if the smoothing parameter is selected based on standard deviation only. 2- cross-validation is very time-consuming[69].

Another way to approach the problem of 'smoothing parameters' is to aggregate training data and approximate the conditional probabilities of the class by Gaussian functions centered at group points rather than actual training points. The data aggregation gives additional ability to estimate the smoothing coefficients of these 'Gaussian functions' as standard deviations within the group[70]. Therefore, how to choose the

smoothing parameter is critical to its direct effect on network resolution.

A 'PNN' is an implementation of a statistical algorithm called kernel discriminant analysis in which the operations are organized into a multilayered feed-forward network with four layers.

1- Input layer: The input layer contains the nodes with a set of measurements. Each neuron in the input layer represents a predictor variable. In categorical variables, 'N-1' neurons are used when there is an N number of categories. It standardizes the range of the values by subtracting the median and dividing by the interquartile range. Then the input neurons feed the values to each of the neurons in the hidden layer.

2- Pattern layer: The pattern layer consists of the 'Gaussian functions' formed using the given set of data points as centers. This layer contains one neuron for each case in the training data set. It stores the values of the predictor variables for the case along with the target value. A hidden neuron computes the Euclidean distance of the test case from the neuron's center point and then applies the RBF kernel function using the sigma values.

$$f_A(\mathbf{X}) = \frac{1}{(2\pi)^{p/2}} \frac{1}{\sigma^p} \frac{1}{m} \sum_{i=1}^m \exp\left[-\frac{(\mathbf{X} - \mathbf{X}_{Ai})^t (\mathbf{X} - \mathbf{X}_{Ai})}{2\sigma^2}\right] \quad (2.16)$$

where

$i =$ pattern number.

$m =$ total number of training patterns.

$X_A =$ i th training pattern.

$\sigma =$ smoothing parameter.

$p =$ dimensionality of measurement space.

Note that ' $f_A(X)$ ' is simply the sum of small multivariate Gaussian distributions centered at each training sample. However, the sum is not limited to being Gaussian. It can, in fact, approximate any smooth density function.

3- Summation layer: The summation layer performs a sum operation of the outputs from the second layer for each class.

4- Output layer: The output layer performs a vote, selecting the largest value. The associated class label is then determined[71]. The PNN architecture is shown in Figure(2.16).

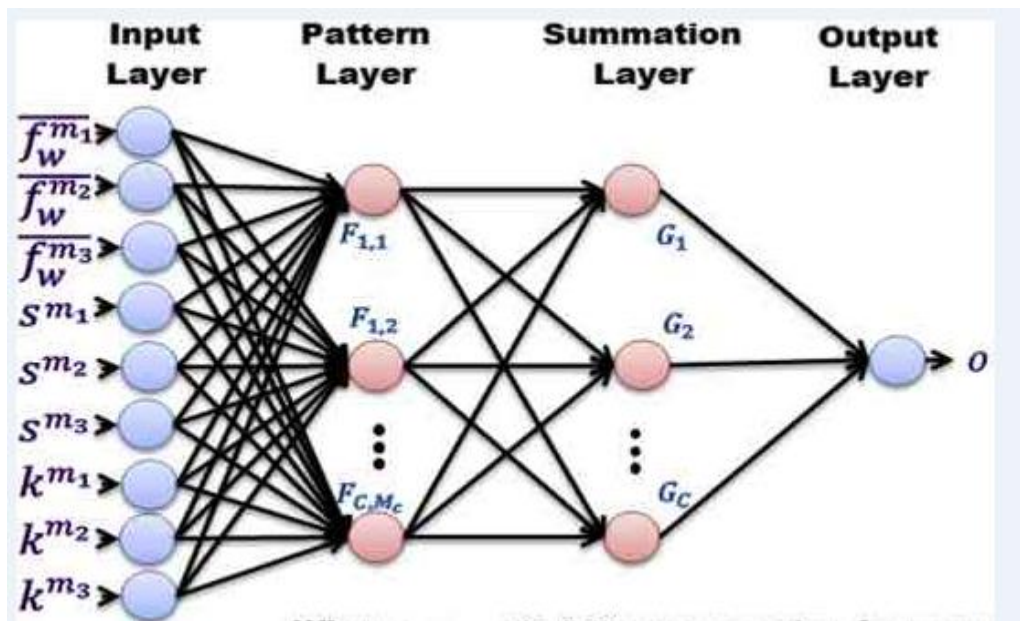


Figure (2.16) Architecture of PNN[68]

2.7.3 Genetic Algorithm(GA)

EC is a family of optimization algorithms that are inspired by biological evolution such as Genetic algorithm, survival of creatures such as Genetic algorithm, Particle Swarm Intelligence, Ant Colony Optimization, Artificial Bee Colony optimization, etc. or any biological processes. They have been applied to image registration problems recently. Dasgupta and McGregor proposed a structured GA for automatic registration of digital images[72].

Registration using genetic algorithm is a fast process and provide. computationally accurate genetic algorithm is applied on any image to get the new enhanced results [73] The output image is greatly better than its original that contains the parents' features. The fine details of a degraded image can be extracted through image enhancement

techniques that also improve the quality of a given image[74].

The natural evolution theory "Darwinian Evolution" represent the basic principle of 'GA'. They mimic the survival of the fittest among a group. Figure (2.17) illustrates a standard flowchart of a generic algorithm. The term generation refers to the single iteration of the algorithm. The simplest form of 'GA' is comprehensive, and wide range of aspects can be implemented variously depending on the problem (e.g. representation of solution (chromosomes), type of encoding, selection strategy, type of crossover and mutation operators, etc.) [75].

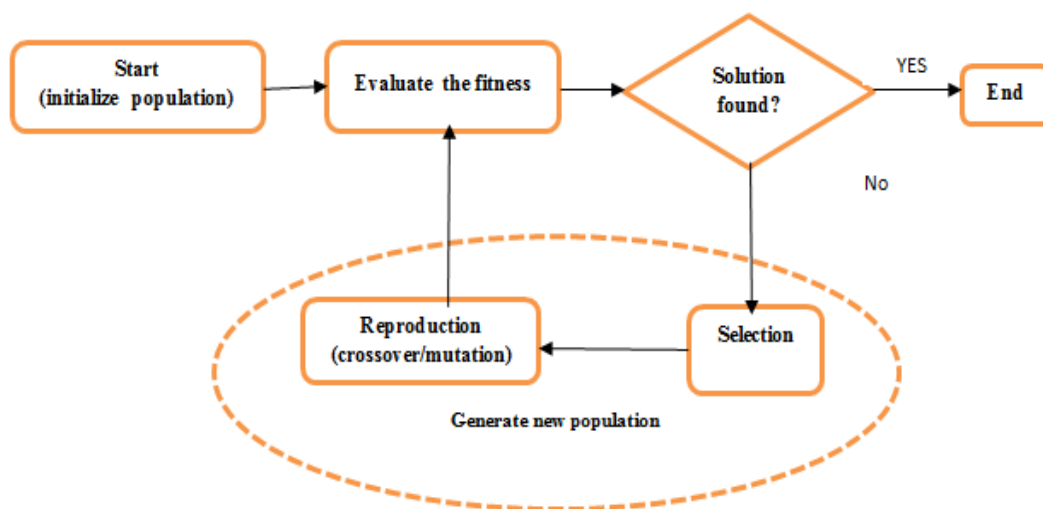


Figure (2.17) Flowchart of Basic Genetic Algorithm Iteration.[75]

Every optimization problem depends essentially on the fitness function. The optimization method can do no help in finding a solution if the fitness function was ineffective. Hence, choosing a fitness function

represent a challenging selection. The permanence of the chromosomes in the populations is analyzed by 'GA' through the 'fitness function'. According to a given problem, fitness evaluation functions are either sophisticated or simple. The operators of Genetic algorithms[76]:

1- Selection: The process of selecting parents' chromosomes of the next generation from the current one is performed by the selection operator. Due to "Darwinian Evolution", the new offspring is created by the best ones that survive. Parents are selected in pairs. Selecting chromosomes can be achieved through different methods[77]:

a- Uniform Selection: In the parents, in this selection method, are chosen in a random manner out of a uniformed distribution through the use of several parents and expectations. This results in an undirected search.

b- Roulette Wheel Selection: This is a stochastic method, where individual having higher fitness value have more chances to select. This is the most common selection method used in GAs. They were used in the proposed system. If f_i is the fitness of individual i in the population, its probability of being selected is:

$$p_i = \frac{f_i}{\sum_{j=1}^N f_j} \quad (2.17)$$

Where

N is the number of individuals in the population.

f_i is the fitness of individual i in the population

c- Tournament Selection: It provides selection pressure by holding a tournament among s competitors, where s is tournament size. The individual that holds the highest fitness of tournament competitors is the winner of tournament. Then, the winner is inserted into mating pool. The mating pool comprise of tournament winner, has a higher fitness value than average population fitness.

2- Crossover: a simple crossover process may take a place after reproduction. This process is made of two steps: in the first member of the recently reproduced strings in the mating pool are randomly mated. Secondly, a crossing over is performed on each pairs of chromosomes. Following different types of crossing over are explained[78]:

a- Single Point Crossover: Crossover position is selected between one and $(L-1)$ randomly, where L is the length of chromosome. Two parents are crossed at that point. First child in this crossover is identical to first parent up to the crossing point and identical to the second parent after the crossover point.

b- Two Point Crossover: In two points crossover, two crossover positions are randomly selected between one and $(L-1)$, where L is

the length of chromosome and two parents are crossed at those points.

3- Mutation: Mutations are global searches. A probability of mutation is again predetermined before the algorithm is started which is applied to each individual bit of each offspring chromosome to determine if it is to be inverted. As new individuals are generated each character mutated with given probability P_m . In simple GA, mutation means a 1 to a 0 and vice versa with mutation probability. Figure(2.18) shows stages of chromosome before and after mutation[79].

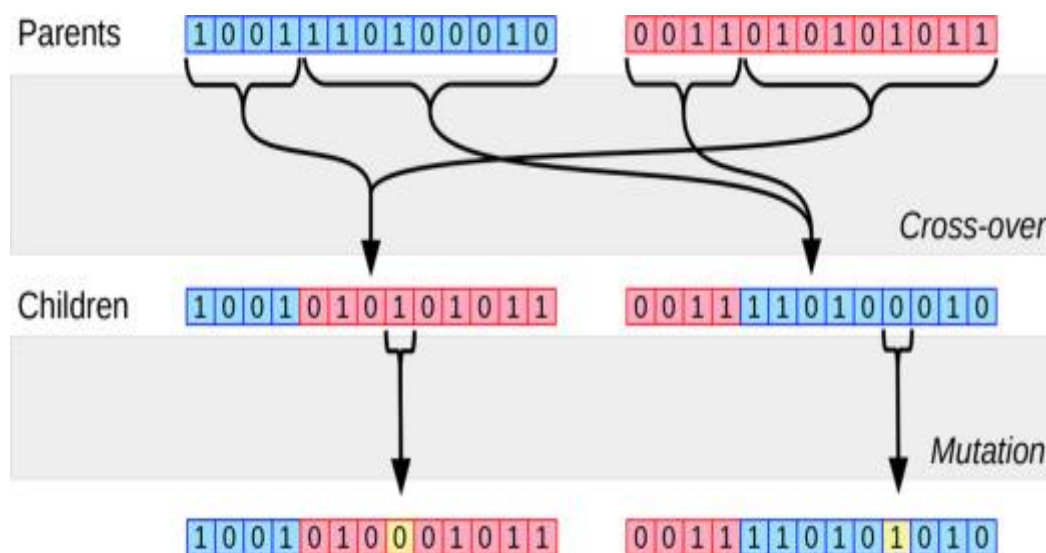


Figure (2.18) Crossover and Mutation Operator[79]

2.8 Performance Measurement

One of the most popular arrays in machine learning is used to test the performance of algorithms. It contains information and details about the actual (human-classified) classifications and the predictive classifications that the classifier predicts. Each column in the array represents the Predicted class and each row represents the actual class. Workbook performance is usually evaluated using the data in the matrix, and its size depends on the number of categories. As shown in the Table (2.4), [80].

Table (2.4) Confusion Matrix

confusion Matrix		Predicated	
		Normal	Abnormal
Actual	Normal	True Positive (TP)	False Negative (FN)
	Abnormal	False Positive (FP)	True Negative (TN)

- 1- True positive (TP): Test result is one that detects the condition condition is present.
- 2- True negative (TN): Test result is one that does not detect the condition when the condition is absent.
- 3- False positive (FP): Test result is one that detects the condition when the condition is absent.
- 4- False negative (FN): Test result is one that does not detect the condition when the condition is present.

Precision is the ratio of true positive to all positive forecasts used as accuracy, precision, recall and F-measurement as the output measures shown in Table (2.5). The model with the highest accuracy is the lowest number of false positives. Selectivity is the consistency of the reaction to some other material without intervention. Sensitivity is a measure of the share of real negative cases expected to be negative (or true negative). Recall or the true positive rate is the measure for how many true positives get predicted out of all the positives in the dataset. It is sometimes also called sensitivity. When minimizing the number of false negatives, be chosen the model with the highest value of Recall[81].

Accuracy the ratio of correct predictions to the total number of predictions. When there is a neutralization the question of false positives versus false negatives, Be chosen the model with the highest accuracy. 'F-Measure' is the harmonic mean(average) of the precision and recall 'F1 Score' is best if there is some sort of balance between precision and recall in the system. Oppositely F1 Score isn't so high if one measure is improved at the expense of the other[81].

Table (2.5) Classification Performance Measurement

Measure	Formula	NO. of Equation
Precision	$\text{Precision} = \frac{TP}{TP+FP}$	(2.18)

Recall / Sensitivity	$\text{Recall / Sensitivity} = \frac{TP}{TP+FN}$	(2.19)
Selectivity	$\text{Selectivity} = \frac{TN}{FP+TN}$	(2.20)
Accuracy	$\text{Accuracy} = \frac{TP+TN}{TP+TN+FP+FN}$	(2.21)
F-Measure	$\text{F-Measure} = \frac{2 * \text{Precision} * \text{Recall}}{\text{Precision} + \text{Recall}}$	(2.22)

2.9 Transmission Model(Arduino and GSM)

Arduino is an open source platform used to build and program electronics that can receive and Send information to most devices, through Internet to command the specific electronic device.it uses a hardware called Arduino Uno. Circuit board and software Simplified C ++ [82] for programming the board. These modern days. Arduino is frequently used in microcontroller programming for ease of setup and ease of use, like any microcontroller it is a circuit board with a chip that can be programmed to perform a large number of tasks, it sends information from computer program to Arduino microcontroller. Finally to the specified circuit or machine with multiple circuits in order to execute the specified command[83]. The features of the various types[84] of Arduino boards are listed in the Table (2.6) and Figure (2.19).

Table (2.6): The Type of Arduino

Arduino Board	Processor	Memory	Digital I/O	Analogue I/O
Arduino Uno	16Mhz ATmega328	2KB SRAM, 32KB flash	14	6 input, 0 output

**Figure (2.19)** Types of Arduino Boards[82]

Global System for Mobile Communication (GSM). It is a digital cellular technology used for transmitting mobile voice and data services. GSM makes use of narrowband Time Division Multiple Access (TDMA) technique for transmitting signals. It was developed using digital technology. It has an ability to carry 64 kbps to 120 Mbps of data rates. GSM provides basic and advanced voice and data services, including roaming. It is the ability to use a GSM phone number in another GSM network. GSM digitizes and compresses data, then sends it down a channel with two other streams of user data, each in its own time slot. It

operates at either the 900 megahertz (MHz) or 1,800 MHz frequency band[85].

Using Arduino with GSM, this ability allows to do most of the operations that can be performed using a GSM phone: making and receiving voice calls, sending and receiving short messages, and connecting to the Internet via the GPRS network. GSM Shield contains a modem that transfers data from a serial port to a GSM network. The modem performs operations via a series of AT commands. The library extracts low-level connections between modem and SIM card. It is based on the serial software library to communicate between modem and Arduino. Typically, each individual command is part of a larger chain necessary to perform a specific function. The library can also receive information and return it when necessary[86].

CHAPTER THREE

A SOFT COMPUTING MODEL FOR IMAGE REGISTRATION AND CLASSIFICATION

3.1 Introduction

The design includes the proposed automatic classification system based on the soft computing paradigm. The design steps are explained in terms of the techniques, algorithms and tools that have been used.

3.2 The Proposed Automatic Classification System

The proposed system automates the process of classification. Several MRI images are acquired for the patient's brain at different views, location, and times. The system then relates these images together to make one complementary image be more useful than the original images and preparing it for analysis using the image registration process. The produced model image is then forwarded to the classification model for the prediction task leads to the final decision, whether it was normal or abnormal. After that, the classification result sent via a transmission model to the patient. The proposed system includes three main models. The first model is an image registration that includes the genetic algorithm. The second model of the system is the fuzzy-PNN classifier model. And the transmission model which in turn, composed of two parts, the first is the microcontroller and the second is GSM as in the proposed system Figure (3.1).

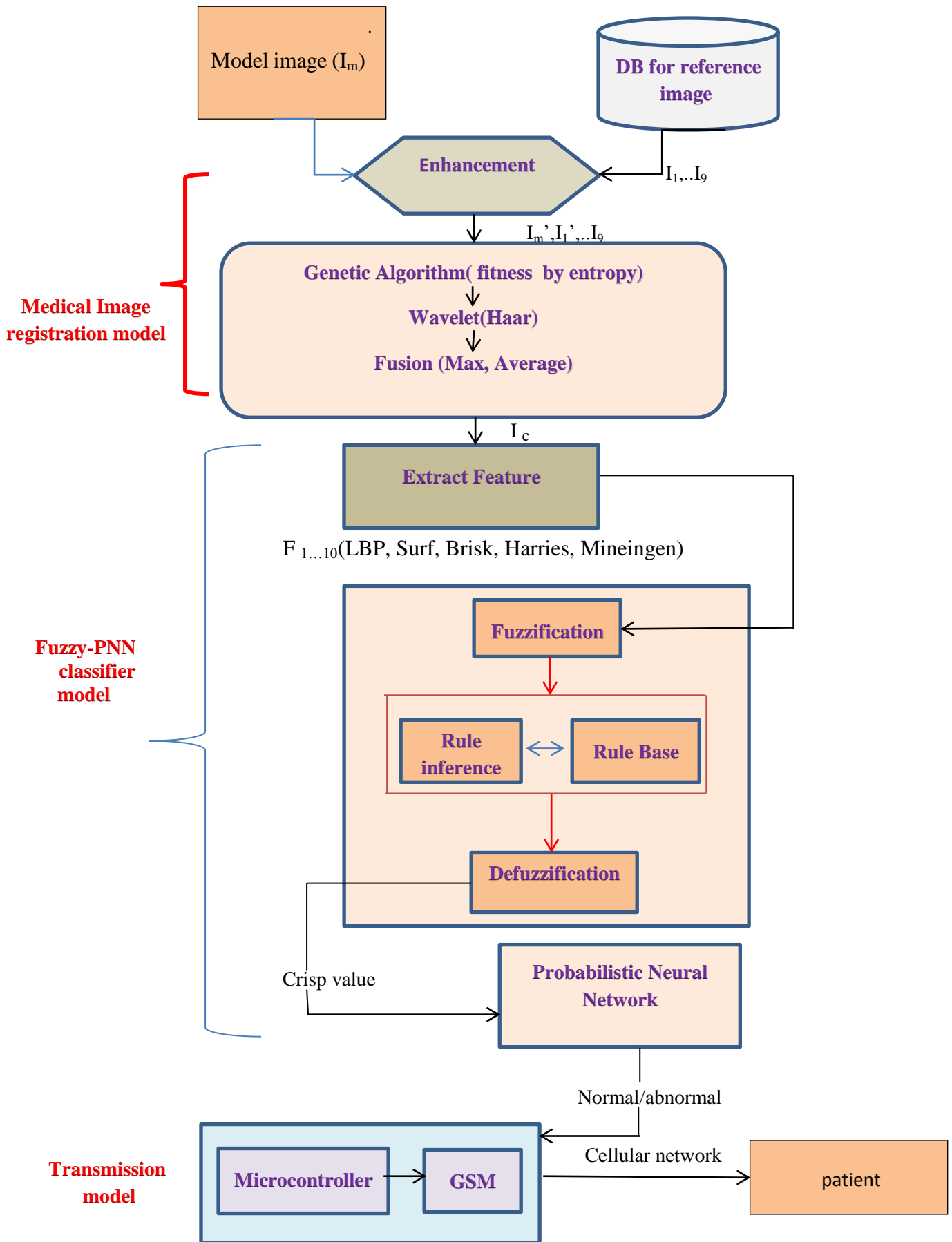


Figure (3.1) Proposed Diagnosis System

below is a detailed explanation of the tools and techniques that have been used in the proposed system:

3.2.1 System Input

The system takes input MRI image from two channels. The first channel is the medical scanning device that produces a model image with complete details for the patient. The second channel is a database which contains 320 images with size 256×256 divided into 180 normal and 140 abnormal photos. as reference images for the patient obtained in different views, times, and location.

3.2.2 Medical Image Registration Model

3.2.2.1 Image Enhancement

The first step in this model is image enhancement. Remove noise from the input image help in the accurate analysis. A Gaussian filter was used to enhance the image as in algorithm (3.1).

(3.1) Enhancement Algorithm

Input: model image, 9-reference images

Output: Enhance medical images

for each input image

step1: read the medical Image

step2: set the kernel size (mask of Gaussian) is 3×3

step3: set the parameter standard deviation($\sigma= 0.2$).

step 4:produced a Gaussian filter kernel according to Equation (2.10).

step 5:applying a convolving the image with a Gaussian function

Retune Enhance images

3.2.2.2 GA Optimizer

The enhanced images forwarded to the genetic algorithm for applying the registration process and produce a single complementary image with all details. The necessary step in the IR, which are the transformation, similarity metric, and optimizer implemented inside the GA. The setting of the algorithm was as described below:

A- Initial population: This consists of 10 images, each of which is considered a chromosome. The length of the chromosome represents the length of the image itself: 256 x 256.

B- Fitness Value: In this step, the fitness value of each chromosome is calculated relying on the entropy, using entropy Equation(3.1) and (3.2).

$$P = \frac{k_j}{s} \quad (3.1)$$

K_j , the number of sequence of gray level (0-255), s size of image
(256× 256)

$$\text{Entropy}(i) = - \sum_{j=0}^{255} p_j \log_2 p_j \quad i=(1-10) \quad (3.2)$$

C- Selection: Here two chromosomes are selected at a time by the roulette wheel. Which is divided into several sections and choose a fixed point on the circumference of the wheel, then choose the area of the wheel that comes in front of the fixed point as one of the parents, and the same process is repeated for the second parent according to their fitness. The chromosome with the highest fitness is considered the better ,therefore, the chance to choose it increases. Using Equation No.(2.17).

D- Crossover: The image that exits the selection phase enters to crossover for the purpose of conducting transformed using DWT(Haar), then combined using the fusion operation with two basic operation, the maximum in Equation (3.3). And average in Equation(3.4). In this step, the transformation stage from the IR was applied. The Figure(3.2) indicates an example illustrating the maximum and average process in crossover.

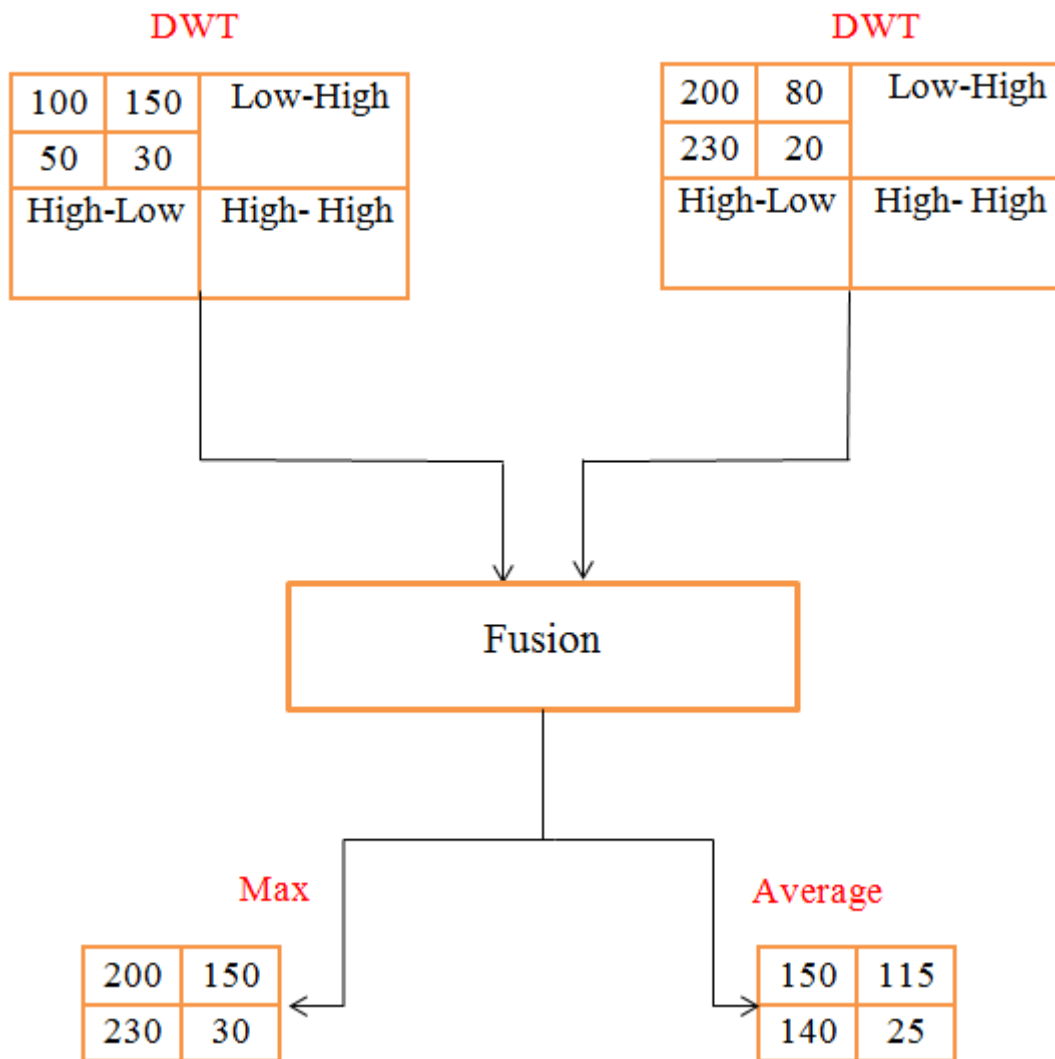


Figure (3.2) Diagram of the Crossover

The maximum equation

$$Xi = \text{Max} (p_{ia}, p_{ib}) \quad (3.3)$$

The proposed average equation

$$Xi = \frac{p_{ia} + p_{ib}}{2} \quad (3.4)$$

Where X is image fusion , p is pixel and i is image.

E- Terminating condition: The Terminating condition Equation (3.5) checks the candidate solution for each generation and formulated as follow:

$$T = \text{Fit}(\text{DWL}(I_s)) - \text{Fit}(\text{DWL}(I_m)) \quad (3.5)$$

Where:

T: Terminating condition for the current image

Fit: fitness value for image

I_m: model image

I_s: refrence image

F- Stopping condition: The algorithm stops when the $T=0$ which mean find the candidate solution. These details can be summarized in GA algorithm as follows (3.2).

(3.2) Genetic Algorithm**Input: 9- reference images , model image****Output: 10-complementary images****step1: set $P = 10$, calculate their fitness value****step 2: for each chromosome in P do :****step2.1:apply roulette wheel selection to generate S population Using Equation No.(2.17).****step 2.2: apply DWT to selected chromosome in S and fusion crossover to generate C population by Equation (2 .11) , (2.12).****step 2.3: calculate fitness value for C ,****step2.4: check stopping condition using Terminating Equation(3.5), if $T= 0$ or max iteration then return C_i otherwise continue****3.2.3 Fuzzy- PNN classifier Model****3.2.3.1 Features Extraction**

The features extraction is applied to the 10- complementary model image to extract features that include (closed boundary regions, edges, contours, line intersections, corners). The operations (LBP, SURF, BRISK, Eigenvalue, and Harris) are used to produce the best 10 feature for each image assessing in the classification stage.

The MRI image of the brain is divided into two parts, IT representing the right part and IL representing the left part. Then the features are extracted from the right and left part of the image that was divided by applying five algorithms that represent each of the fuzzy set (LBP, SURF, Brisk, Harris, Mining). The best and robust ten extracted features of an image are obtained from the subtraction between every two

parts for the image as in subtraction Equation(3.6). When dividing the image into two parts, the normal parts of the human brain are equal, but in the case of a tumor, damage, or anything abnormal, there is a difference in the right part from the left part, so a subtraction process was used to discover and determine the tumor Then the summation process Equation(3.7) is applied to get a final result.

$$M_F = F(I_L) - F(I_T) \quad (3.6)$$

Where:

M_F : The matching result complementary model- image for specific extraction method, F : function of extraction like LBP,ect.

$$SM = \sum_{i=1}^{10} Mf_i \quad (3.7)$$

Where:

SM : is the sum of subtraction, i : feature number.

(3.3) Features Extraction Algorithm**Input:** 10- complementary model image**Output:** SM_i **For each input image i do:****Step1:** divide image I into I_L, I_T **Step2:** extract feature for both I_L, I_T using LBP, Brisk, Harries, Surf, Minegine Equation in (2.1),(2.2),(2.3),(2.4),(2.5),(2.6),(2.7),(2.8) and (2.9)**Step3:** compute M_F **Step4:** compute SM**Return(SM)****3.2.3.2 Fuzzy Inference System**

The FIS combine 5 different image features (LBP, Brisk, Harries, Surf, Minegine) yield compound feature that represents them. It takes the output from the MIR model which represents a 5- vector of crisp value, and then it approximates one output value for each input vector. Then forward it to the PNN for further classification.

a. Fuzzification

5- input vector of integer value was converted into 5-fuzzy sets. Each fuzzy set element $x \in R, x = \{0, \dots, 255\}$ and one output fuzzy set.

These fuzzy sets represented as linguistic variable LBP, Surf, Brisk. Harries and Minengine for input set and Quality for output set. The linguistic fuzzy term {low, high } for all input sets and {low, medium, high} for output set as follow:

$F_{LBP} = \{low, high\}$, $F_{SURF} = \{low, high\}$, $F_{BRISK} = \{low, high\}$, $F_{Harries} = \{low, high\}$, $F_{mineigenvalue} = \{low, high\}$.

Figure (3.3) Illustrates membership function for the fuzzy sets and had the shown user defined membership function:

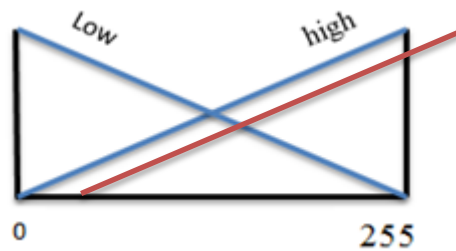


Figure (3.3) Membership Function for The Fuzzy Sets

$$Low(x) = \begin{cases} \frac{255 - x}{255} & \text{if } 0 \leq x \leq 255 \end{cases}$$

$$High(x) = \begin{cases} \frac{x}{255} & \text{if } 0 \leq x \leq 255 \end{cases}$$

The output set is:

$F_{Quality} = \{low, medium, high\}$

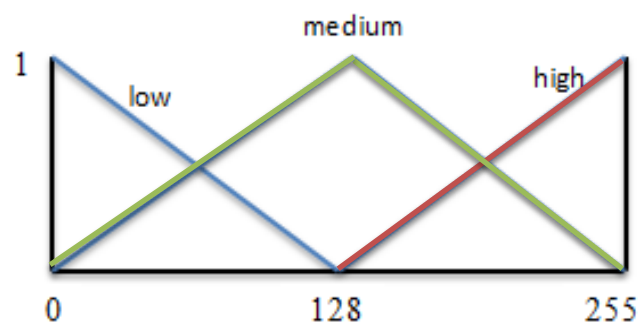


Figure (3.4) Output of the Fuzzy Set

Figure (3.4) shows this fuzzy set and the user defined membership function for each linguistic term is shown below:

$$Low(x) = \begin{cases} \frac{128 - x}{128} & \text{if } 0 \leq x \leq 128 \end{cases}$$

$$High(x) = \begin{cases} 1 & \text{if } x = 255 \\ \frac{x}{255} & \text{if } 128 < x < 255 \\ 0 & \text{if } x = 128 \end{cases}$$

$$Medium(x) = \begin{cases} 1 & \text{if } x = 128 \\ \frac{x}{128} & \text{if } 0 < x < 128 \\ \frac{(128 - x)}{128} & \text{if } 128 < x < 255 \end{cases}$$

b. Rule Base and Inference

The generated rule or knowledge base considering different combinations of input fuzzy that can be illustrated as follow:

Section1: combine between LBP and Brisk

R1: if LBP is low and Brisk is low then Quality is low

Also

R2: if LBP is high and Brisk is low then Quality is medium

Also

R3: if LBP is low and Brisk is high then Quality is medium

Also

R4: if LBP is high and Brisk is high then Quality is high

Section2: combine between LBP and Surf

Also

R5: if LBP is low and Surf is low then Quality is low

Also

R6: if LBP is high and Surf is low then Quality is medium

Also

R7: if LBP is low and Surf is high then Quality is medium

Also

R8: if LBP is high and Surf is high then Quality is high

Section3: combine between LBP and Harries

Also

R9: if LBP is low and Harris is low then Quality is low

Also

R10: if LBP is high and Harris is low then Quality is medium

Also

R11: if LBP is low and Harris is high then Quality is medium

Also

R12: if LBP is high and Harris is high then Quality is high

Section4: combine between LBP and Mineigin

Also

R13: if LBP is low and Mineigin is low then Quality is low

Also

R14: if LBP is high and Mineigin is low then Quality is medium

Also

R15: if LBP is low and Mineigin is high then Quality is medium

Also

R16: if LBP is high and Mineigin is high then Quality is high

Section5: combine between Brisk and Surf

Also

R17: if Brisk is low and Surf is low then Quality is low

Also

R18: if Brisk is low and Surf is high then Quality is medium

Also

R19: if Brisk is high and Surf is low then Quality is medium

Also

R20: if Brisk is high and Surf is high then Quality is high

Section6: combine between Brisk and Harries

Also

R21: if Brisk is low and Harris is low then Quality is low

Also

R22: if Brisk is low and Harris is high then Quality is medium

Also

R23: if Brisk is high and Harris is low then Quality is medium

Also

R24: if Brisk is high and Harris is high then Quality is high

Section7: combine between Brisk and Mineigin

Also

R25: if Brisk is low and Mineigin is low then Quality is low

Also

R26: if Brisk is low and Mineigin is high then Quality is medium

Also

R27: if Brisk is high and Mineigin is low then Quality is medium

Also

R28: if Brisk is high and Mineigin is high then Quality is high

Section8: combine between Surf and Harries

Also

R29: if Surf is low and Harris is low then Quality is low

Also

R30: if Surf is low and Harris is high then Quality is medium

Also

R31: if Surf is high and Harris is low then Quality is medium

Also

R32: if Surf is high and Harris is high then Quality is high

Section9: combine between Surf and Minengin

Also

R33: if Surf is low and Mineigin is low then Quality is low

Also

R34: if Surf is low and Mineigin is high then Quality is medium

Also

R35: if Surf is high and Mineigin is low then Quality is medium

Also

R36: if Surf is high and Mineigin is high then Quality is high

Section10: combine between Harries and Minengin

Also

R37: if Harris is low and Mineigin is low then Quality is low

Also

R38: if Harris is low and Mineigin is high then Quality is medium

Also

R39: if Harris is high and Mineigin is low then Quality is medium

Also

R40: if Harris is high and Mineigin is high then Quality is high

Inference inside the rule base applied by 5-implication operation listed in Table (2.2).

c. Defuzzification

A mean of maxima method is utilized in this stage to produce the single crisp value for each inference vector. This is done using Equation No. (2.15).

3.2.3.3 PNN Classifier

A probabilistic neural network is a mechanism applied for classifying the incoming output from the FIS. Through the five algorithms, 10 features are extracted from each algorithm. When it enters a stage FIS, these ten features are linked and reduced to only one feature, thus accelerating the learning and training process in the PNN. It consists of four layers as shown in Figure (3.5):

1- Input Layer: 5-input nodes which are integers.

2- Pattern layer: 160 –pattern classified as 70 for abnormal class and 90 for normal class, and a Gaussian activation function.

$$FL(I) = \frac{1}{(2\pi)^{p/2} \sigma^p} \frac{1}{n} \sum_{c=1}^n \times \exp\left[-\frac{(I - I_{LC})^t (I - I_{LC})}{2\sigma^2}\right] \quad (3.8)$$

Where

$c = \text{pattern number}$

$n = \text{total number of training patterns}$

$I_L =$ *ith training pattern from category A*

$\sigma =$ *smoothing parameter*

$p =$ *dimensionality of measurement space.*

3- Summation layer: At the output node for Class k ($k = 1$ or 2 here), all of the Gaussian values for Class k are summed and the sum is scaled so the probability volume under the sum function is unity so that the sum forms a probability density function.

4- Output layer: It takes the output from the summation layer depending on the class of pattern. The class is binary where it gives the final result where output 1 is normal or output 2 is abnormal and then calculates the accuracy of the system. The PNN model goes through two stages, the first of which is a training process through which an accurate system is built, the function of which is to learning phase. Then comes the role of the testing process, which works to diagnose and verify the system to calculate its accuracy.

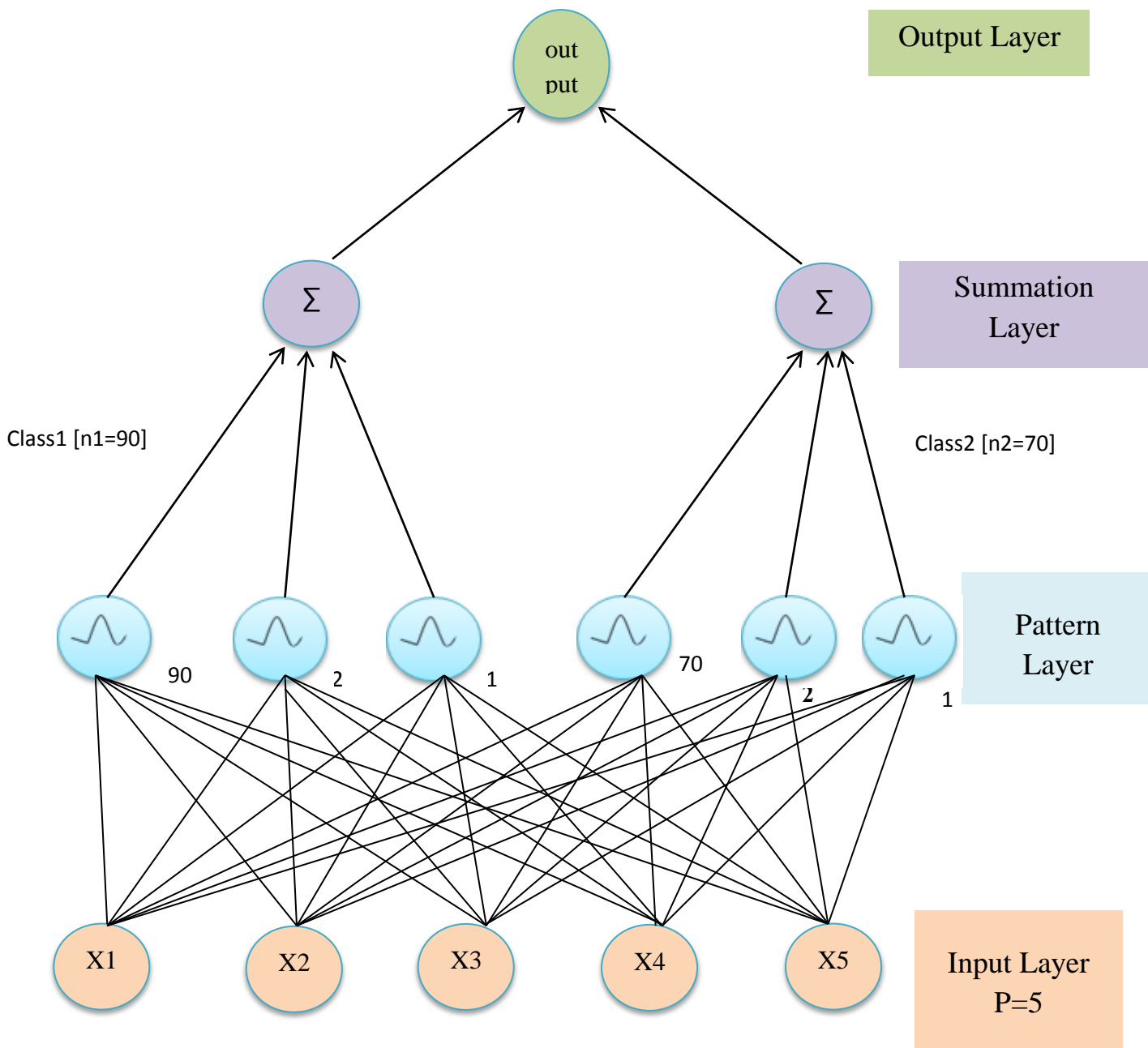


Figure (3.5) The structure of PNN

(3.4) PNN Algorithm (Training process)**Input:** The values of Features extracted that are coming from Fuzzy system**Output:** Building the PNN modelstep1- The input of training samples $\{X^{(k)}\}$, x is 5features 320×0.7 step2- All outputs are assigned $\{d^{(k)}\}$, d is two output (normal, abnormal)

step3- Initialize vector w with small random values

step4- Locate the learning rate $\{\eta\}$ step5- Initial the epoch counter $\{1-100\}$

step6- Repeat the following instruction:

step 6.1- let error = "none"

step 6.2- For all training samples $\{X^{(k)}, d^{(k)}\}$ dostep 6.3- let $u = w^T \cdot X^{(k)}$ step 6.4- when $y = \text{signal}(u)$ step 6.5- if $y \neq d^{(k)}$ then $\begin{cases} w + \eta \cdot (d^k - y) \cdot x^k \\ \text{error} \leftarrow \text{"existent"} \end{cases}$

step 6.6-when epoch = epoch +

(3.5) PNN Algorithm (Testing process)**Input:** Magnetic resonance imaging**Output:** Diagnosis is either normal or abnormalstep1- obtain one sample to be classify $\{x\}$, x is 5features

step2- use vector w adjusted during training

step3- execute the following instruction

step 3.1- let $u = w^T \cdot X$ step 3.2- when $y = \text{signal}(u)$ step 3.3- if $y = 1$ then sample $x \in \{\text{class A}\}$ step 3.4- if $y = 2$ then sample $x \in \{\text{class B}\}$

step4: Return values are either normal or abnormal

3.2.4 Transmission Model

In the proposed system, the transmission model consists of two electronic circuits, the first is the microcontroller and the second is the GSM. The microcontroller, which is an Arduino Uno device, is connected to the computer that acts as a server.

The Arduino receives the results from the server and then sends them to GSM, which searches for the patient's number and sends the result to her via the sim card (SIM) where the patient's mobile is stored. The transmission model as shown in Figure(3.6).

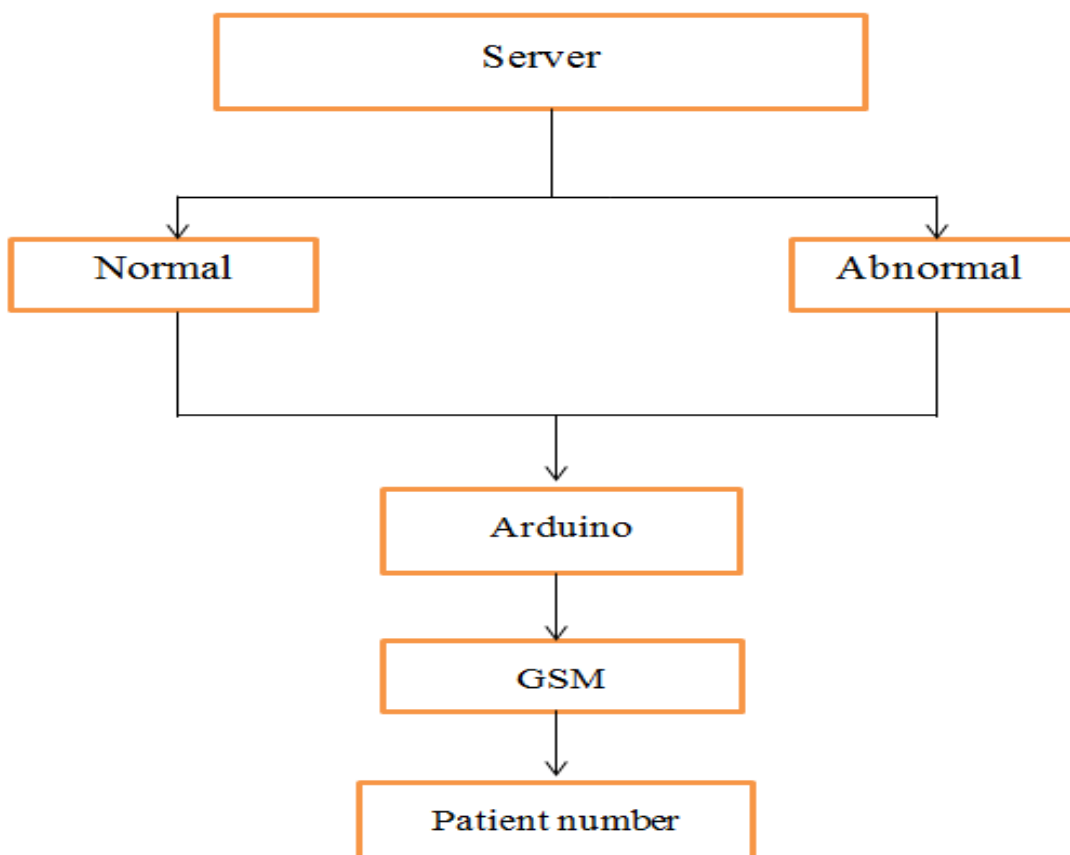


Figure (3.6) Diagram of Transmission Model

(3.6) Transmission Model Algorithm**Input: Diagnostic result (normal or abnormal)****Output: Send the result to the patient's number****step1: Arduino receives data from the server****step2: It is sent to GSM****step3: The GSM searches for the patient's name and number****step4: Send a message with the final result to the patient**

CHAPTER FOUR

IMPLEMENTATION RESULT AND DISCUSSION

4.1 Introduction

This chapter presents the implementation, results and discussion of the proposed system besides the evaluation and limitations .

4.2 Proposed System Implementation

Figure (4.1) shows the deployment diagram for the proposed system.



Figure (4.1) The Deployment Diagram for the Proposed System

In the ideal case, the workflow of the system starts from the clinic where the MRI image is captured by the device. Then the image is forwarded to

the classification application, Then it is sent to the computer for the purpose of processing.

The decision is obtained after running the application and sent via the Arduino and GSM to the patient phones. System specification includes working with one modality of 2D MRI images for brain tumor classification only. Experimental step for hardware and software are shown in the Table (4.1) and Table (4.2).

Table(4.1) Hardware Experimental

Component	Specifications
Server (computer)	<p>HP laptop : Windows 7. Intel (R) Core (TM). i 5 1.60 GHz. The memory 4096 MB RAM , SSD 1Terra</p>
Microcontroller(Arduino)	<p>UNO type . It contains three types of memory:</p> <ul style="list-style-type: none"> 1- flash memory(32 kb) 2- EEPROM(1 kb) 3- SRAM(2 kb) <p>Processor speed is 16MHz. The voltage is 5 and The current maximum is 250 mA.</p>
GSM	<p>It operates at a frequency of 900 MHz. supports data transmission speeds of 9.6 Kbit / s.</p>

Table(4.2) Software Experimental

Component	Description
programming language	Matlab R 2018 b program
Dataset	<p>2D MRI images For the human brain.</p> <p>The total number of photos is 320 divided into 180 normal and 140 abnormal photos.</p> <p>These photos were taken from the site (https://www.kaggle.com/navoneel/brain-mri-images-for-brain-tumor-classification).</p> <p>The samples of data set as shown in Figure (4.2).</p>

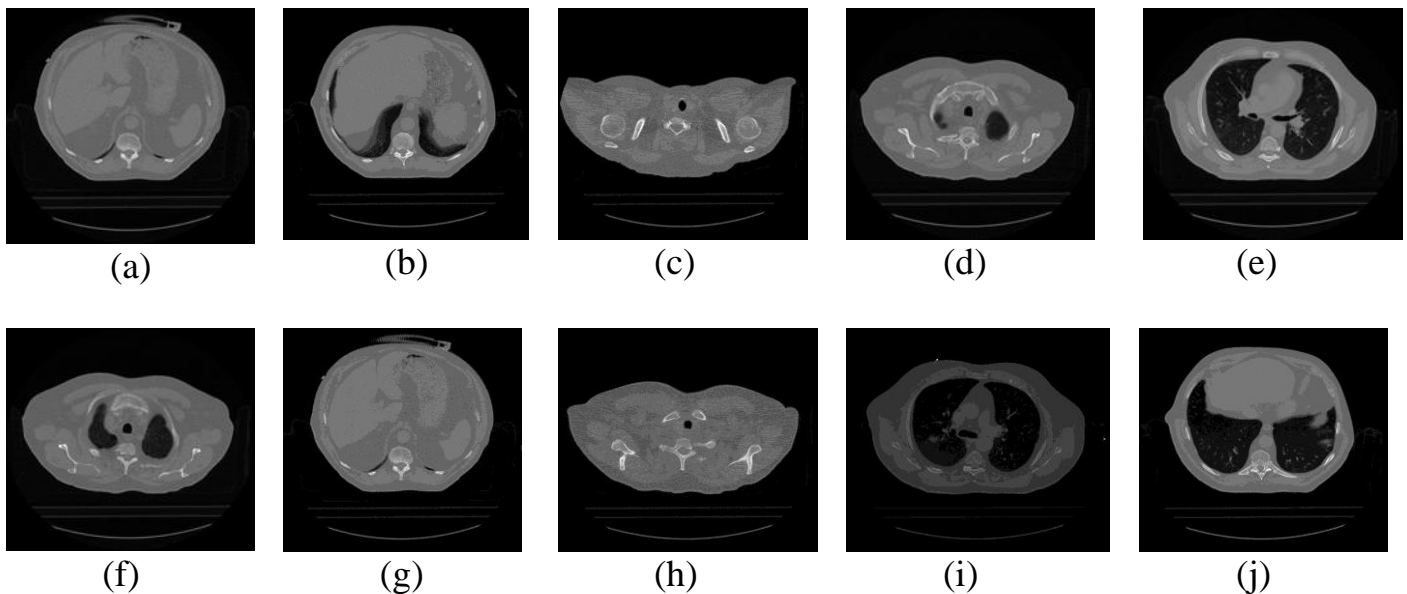


Figure (4.2) The Samples of Data Set (a,b,c,d,e,f,g,h,I, and j) Samples of Different Medical Image

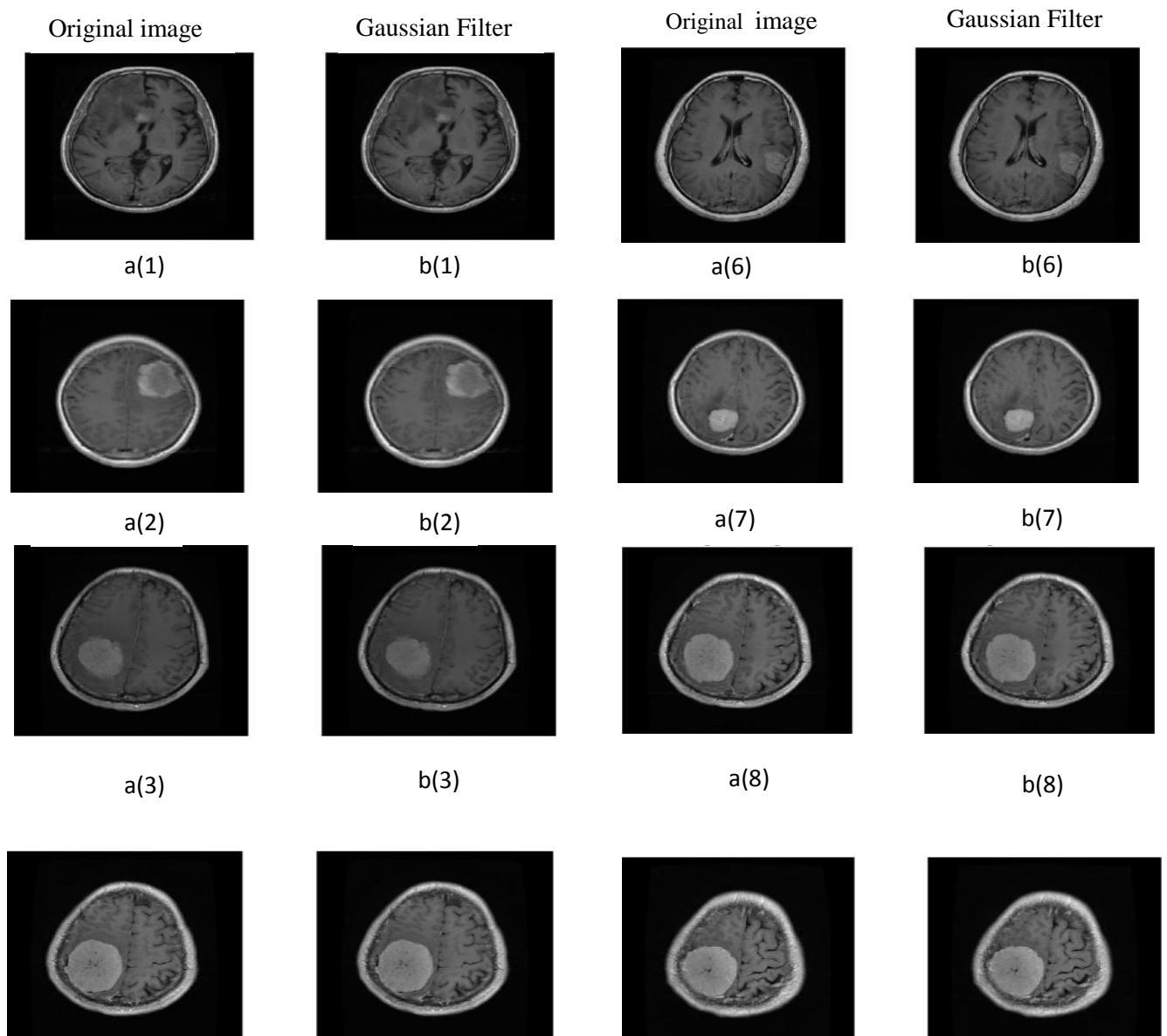
4.3 Proposed System Implementation Results

This section illustrates the implementation results for the proposed system step by step for each model.

4.3.1 Medical Image Registration Model

4.3.1.1 Image Enhancement

This step displays the results of the images after using the Gaussian filter to improve the image and remove noise from it.



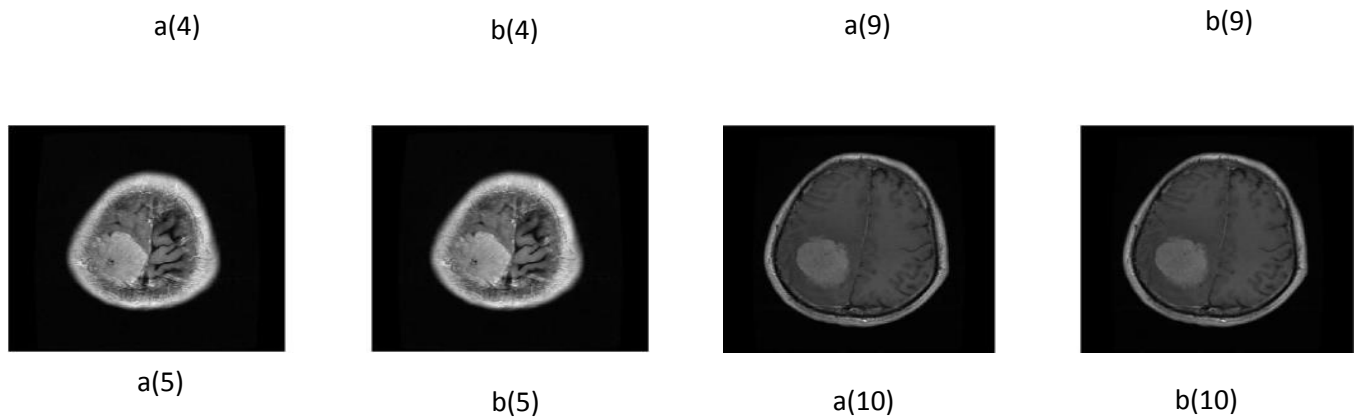
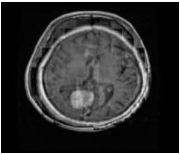



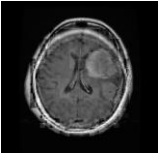
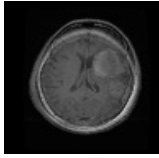
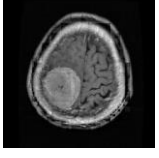
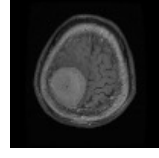
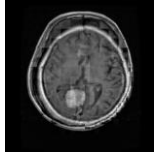
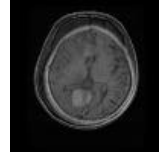
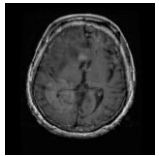
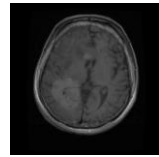
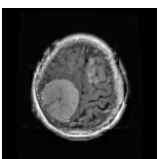
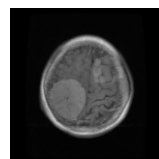
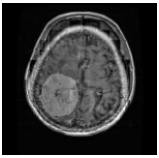
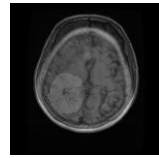
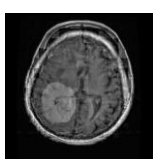
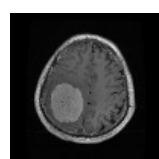
Figure (4.3) Image Enhancement Results (a) Before Enhance and (b) After Enhance

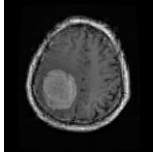
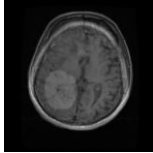
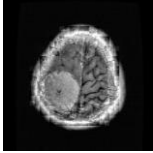
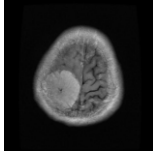
4.3.1.2 GA Optimizer Implementation

A population size of 10 images were selected after many trails, a roulette wheel utilized to elect them for crossover single point type, finally the objective value evaluated between the model image and the crossover population. Table (4.3) gives a detailed explanation for the first generation operation.

Table(4.3) GA Operation for 1st Generation

Selection	Crossover		Fitness		Fitness Max - Modality image	Fitness Average - Modality image
	Fusion Max	Fusion Average	Max	Averag		
1, 4			9.828	8.767	1.115	0.055

3, 2			9.918	9.186	1.205	0.474
10, 8			9.146	8.535	0.434	0.176
1, 4			9.828	8.767	1.115	0.055
10, 1			10.375	9.192	1.663	0.480
3, 8			9.003	8.526	0.288	0.186
1, 7			9.791	8.812	1.079	0.105
6, 6			8.279	8.279	0.432	0.432

1, 6			9.907	8.931	1.195	0.219
5, 6			10.218	8.941	1.506	0.229

The pair (1,4) in the first column indicates the selection of the first image and the fourth image. The second column of the table displays the results of the crossover using fusion. The images obtained by applying fusion maximum are displayed, followed by the images obtained by applying the fusion average. Attention is drawn to the fact that the fusion maximum process gave better results than the fusion average.

As the tumor in the brain often tends to turn white or grey when using the fusion maximum, the brightest areas are highlighted in the images, and thus the affected areas are clearly visible. The third column of the table that shows the results of the fitness values, where the fitness was calculated for the resulting image from the fusion maximum and the fitness calculation for the resulting image from the fusion average.

Through the use of fusion, an image with complementary characteristics was obtained resulting from the combination of two images, which is considered to be the new generation (sons) that has

better characteristics than the parents in the genetic algorithm.

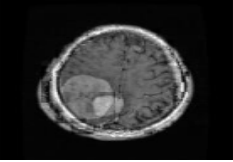
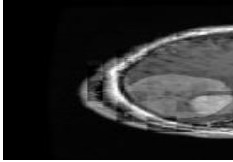
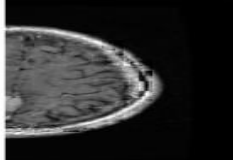
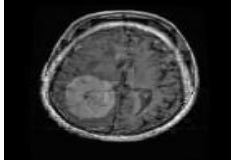
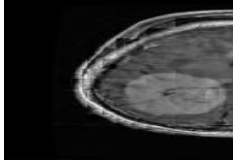
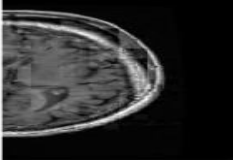
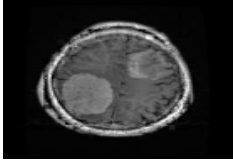
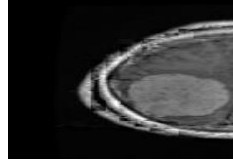
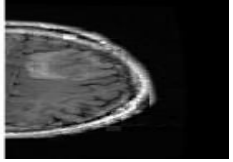
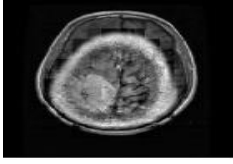
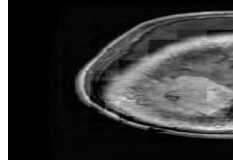
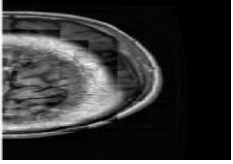
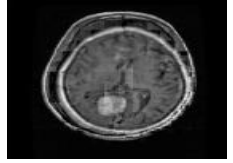
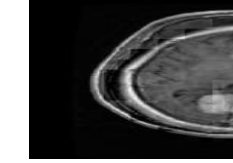
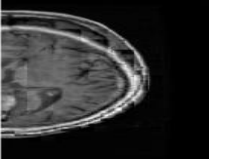
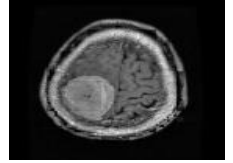
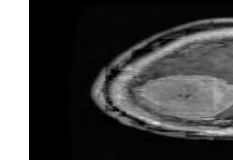
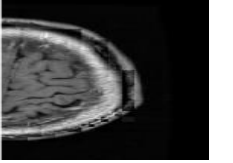
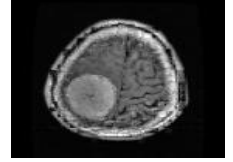
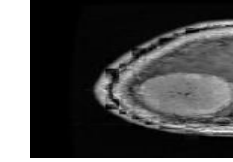
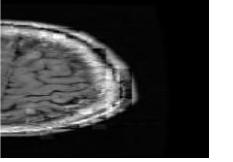
The last column of the table shows the result of subtracting the fitness max from the modality image and the fitness average from the modality image. The candidate image is the best value for fitness. When the subtraction result is zero, this is evidence of obtaining a better fitness image that matches the modality image. While when the value is greater than zero, then, this means that the image is inapplicable i.e. It is of poor fitness, so that image is ignored and another image is tested with characteristics of the modality image. At this stage, the similarity was achieved, which is one of the most important steps of image registration. This process is continuing until 10 candidate images generated.

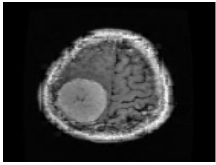
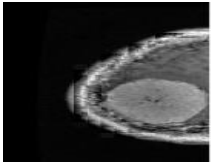
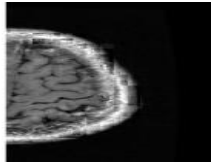
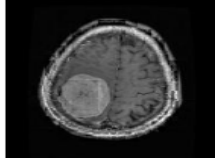
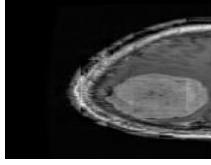
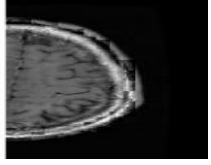
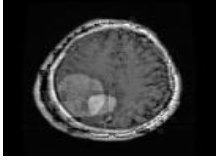
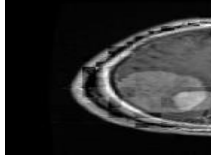
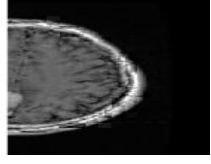
4.3.2 Fuzzy-PNN Classifier Model Implementation

4.3.2.1 Features Extraction Result

The final output from the GA was forwarded to this model for feature extraction process. In this model, the image was divided into two parts, the left and right, and five algorithms were applied (LBP, SURF, BRISK, Mineigen, Harris) to the two parts of the image to extract the features from it, and then a subtraction process was performed between the two parts of the image to notice the changes in that image as shown in the following Tables (4.4) and(4.5) respectively .



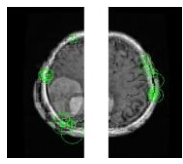
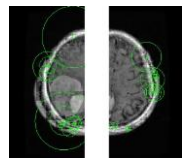
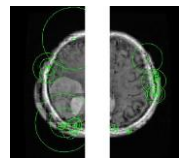
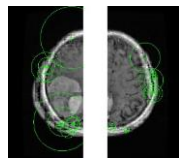
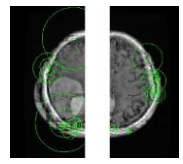
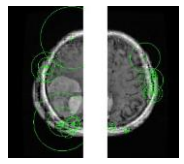
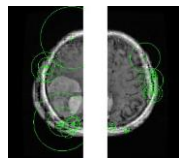
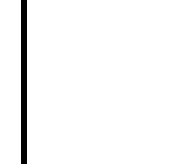


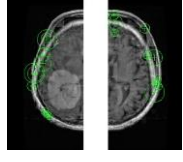
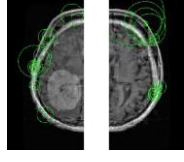
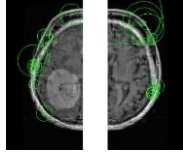
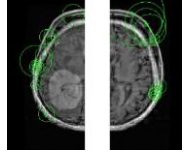
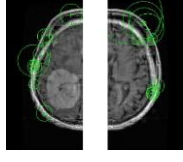
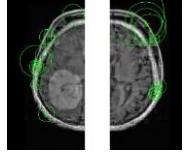
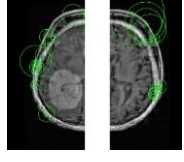
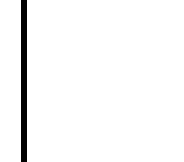
Table(4.4) The Original Image and Its Divisions

Index	The Original Image	Left part	Right part
1			
2			
3			
4			
5			
6			
7			

8		 
9		 
10		 

The second column of Table (4.4) shows the original image, while the third column shows the image after a process of dividing it into two parts right and left parts. Then features are extracted from these two parts.

Table(4.5) The Extract Features from two Parts of the Image

Index	LBP		SURF		BRISK		Mineigin		Harries	
	Left	Right	Left	Right	Left	Right	Left	Righ	Left	Right
1										
2										

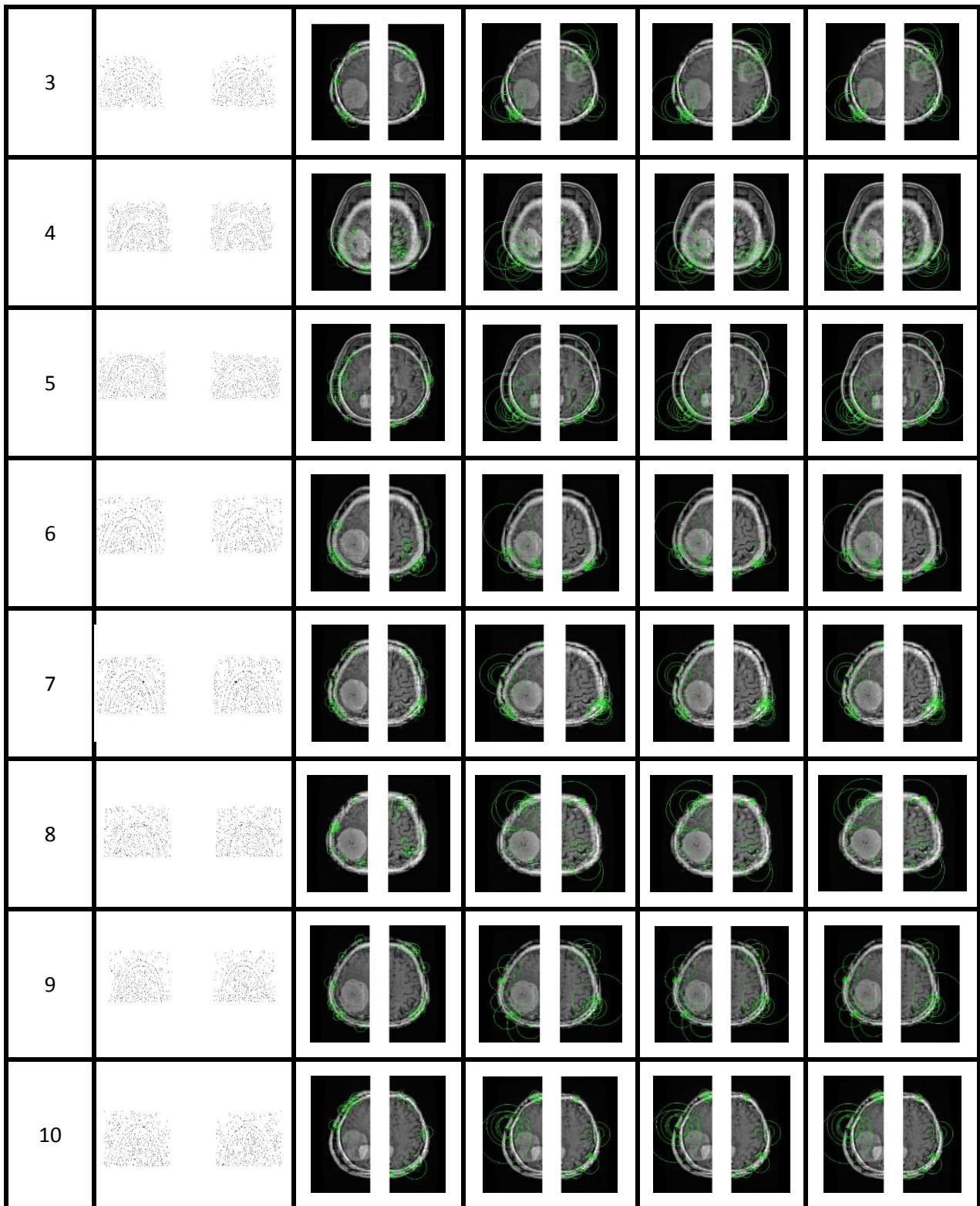


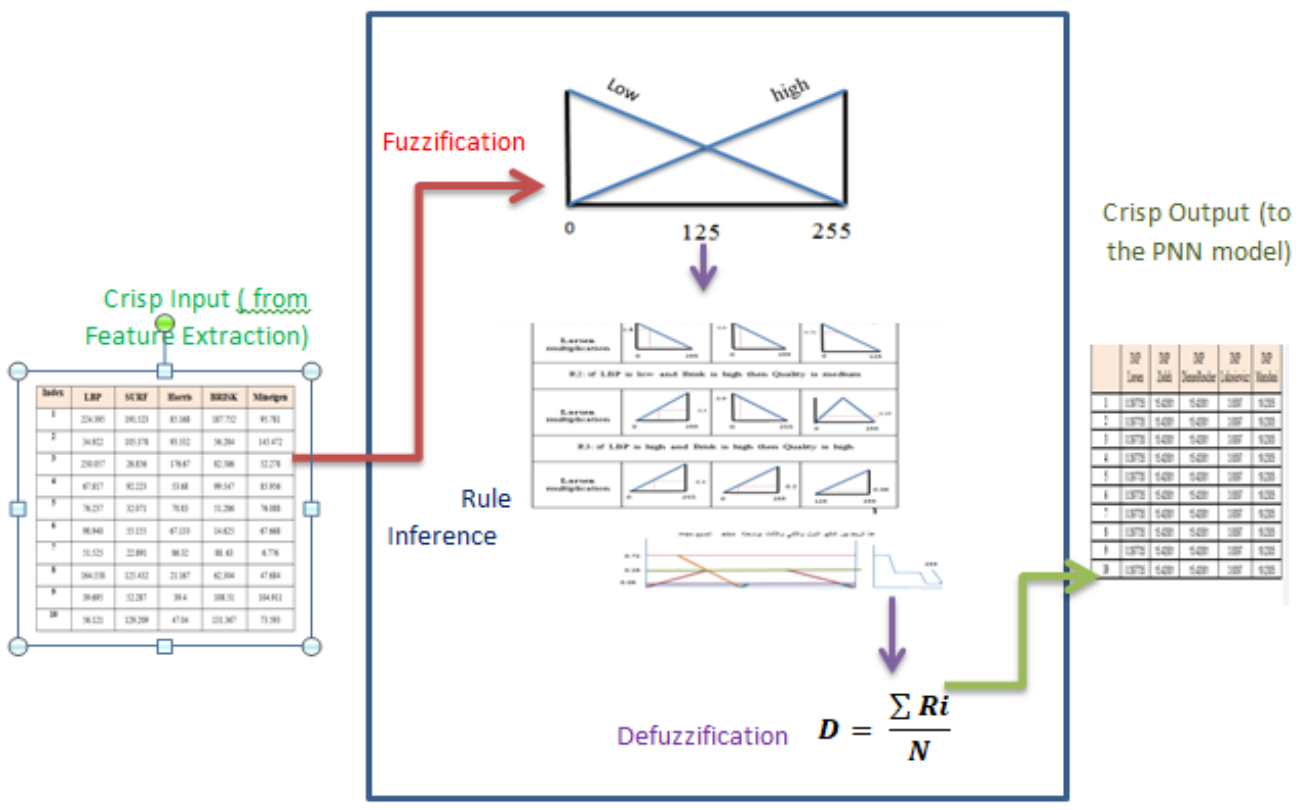
Table (4.5) shows the extracted features using the specified algorithm. The first column shows features extracted by the Local Binary Patterns (LBP) through which a powerful texture classification feature is obtained in a short computational time. Where a texture locally has two complementary aspects, the pattern and its strength.

The second column shows feature extraction when using the Speeded up Robust Feature (SURF) on both parts of the image. The points of interest are revealed, plus a strong and unique description of the extracted features is obtained while increasing the computational speed. The third column of the table shows the extraction of features on the two parts of the image using the Binary Robust Invariant Scalable Key points (BRISK), whose performance lies in discovering the main points, description, and matching. Important information is captured from the image and then that information is distinguished.

The fourth column in the table contains the features extracted from the two parts of the image by applying the Minimum Eigenvalue Algorithm (Min Eigen) through which the corner points are detected as they are based on the calculation of the angle response per pixel. The last column gives the results of the extracted features on the two parts of the image by using Harris Corner Detector focus on the angles of the image. An accurate extraction of corners and infer features of an image are obtained besides extracting the edges and flat. Thus, the most powerful features are obtained by using these algorithms.

4.3.2.2 The FIS Implementation

The complete process for FIS is illustrated in Figure (4.4). The output from the feature extraction is given in Table (4.6) was forwarded to the FIS. Sample of the rule inference is shown in Figures (4.5) ,(4.6),(4,7), (4.8) & (4.9) respectively and finally, the output of the defuzzification step is given in Table (4.7).



Figure(4.4): FIS Workflow

Table(4.6): Feature Extraction Output

Index	LBP	SURF	Harris	BRISK	Mineigen
1	224.395	191.523	85.168	187.752	95.781
2	34.922	105.378	93.332	56.284	145.472
3	250.057	26.856	176.67	82.586	52.278
4	67.817	92.223	53.68	99.547	85.956
5	76.237	32.071	70.83	51.286	76.088
6	98.940	55.155	67.133	14.625	67.668
7	51.525	22.891	86.32	88. 63	6.776
8	164.558	125.432	21.167	62.304	47.684
9	39.695	52.287	39.4	108.51	104.911
10	56.121	129.209	47.04	131.367	73.593

R1: if LBP is low and Brisk is low then Quality is low			
Implication	LBP fuzzy set	BRISK fuzzy set	Quality
Larsen Multiplication			
R2: if LBP is low and Brisk is high then Quality is medium			
Larsen Multiplication			
R3: if LBP is high and Brisk is high then Quality is high			
Larsen Multiplication			
Aggregation	<p style="text-align: center;">y= 50</p>		

Figure (4.5): Part of the Inference Rule(Larsen)

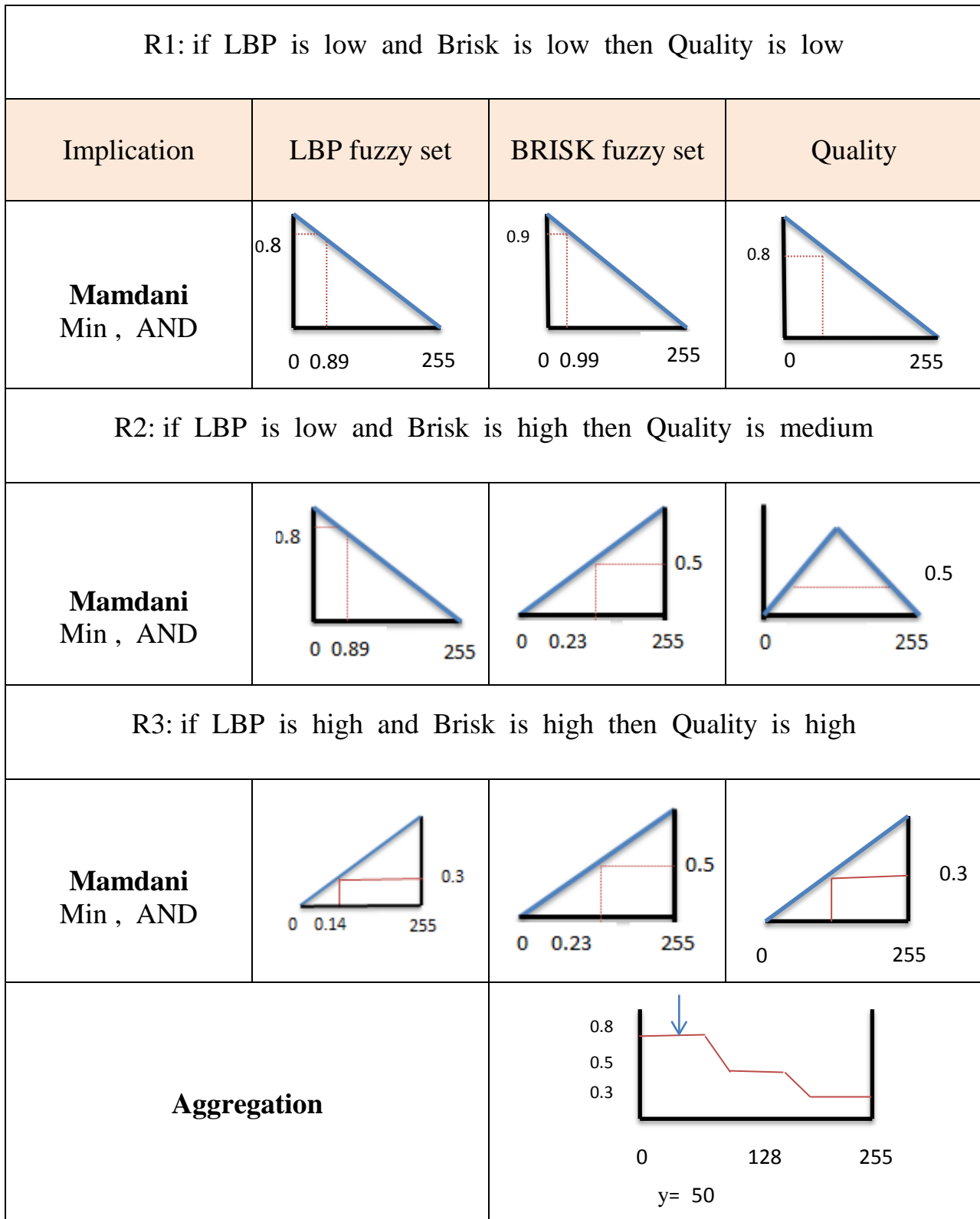


Figure (4.6): Part of the Inference Rule(Mamdani)

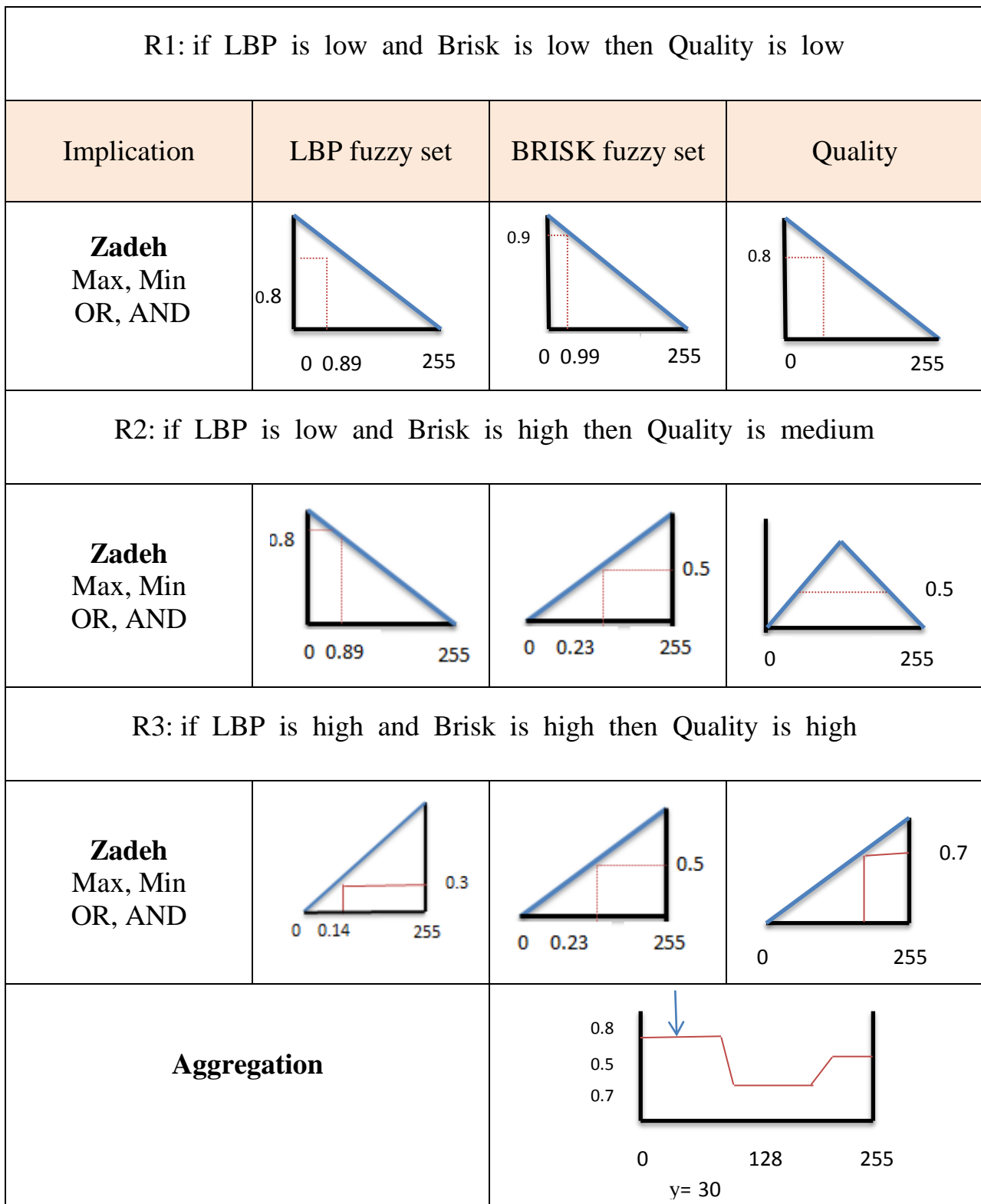


Figure (4.7): Part of the Inference Rule(Zadeh)

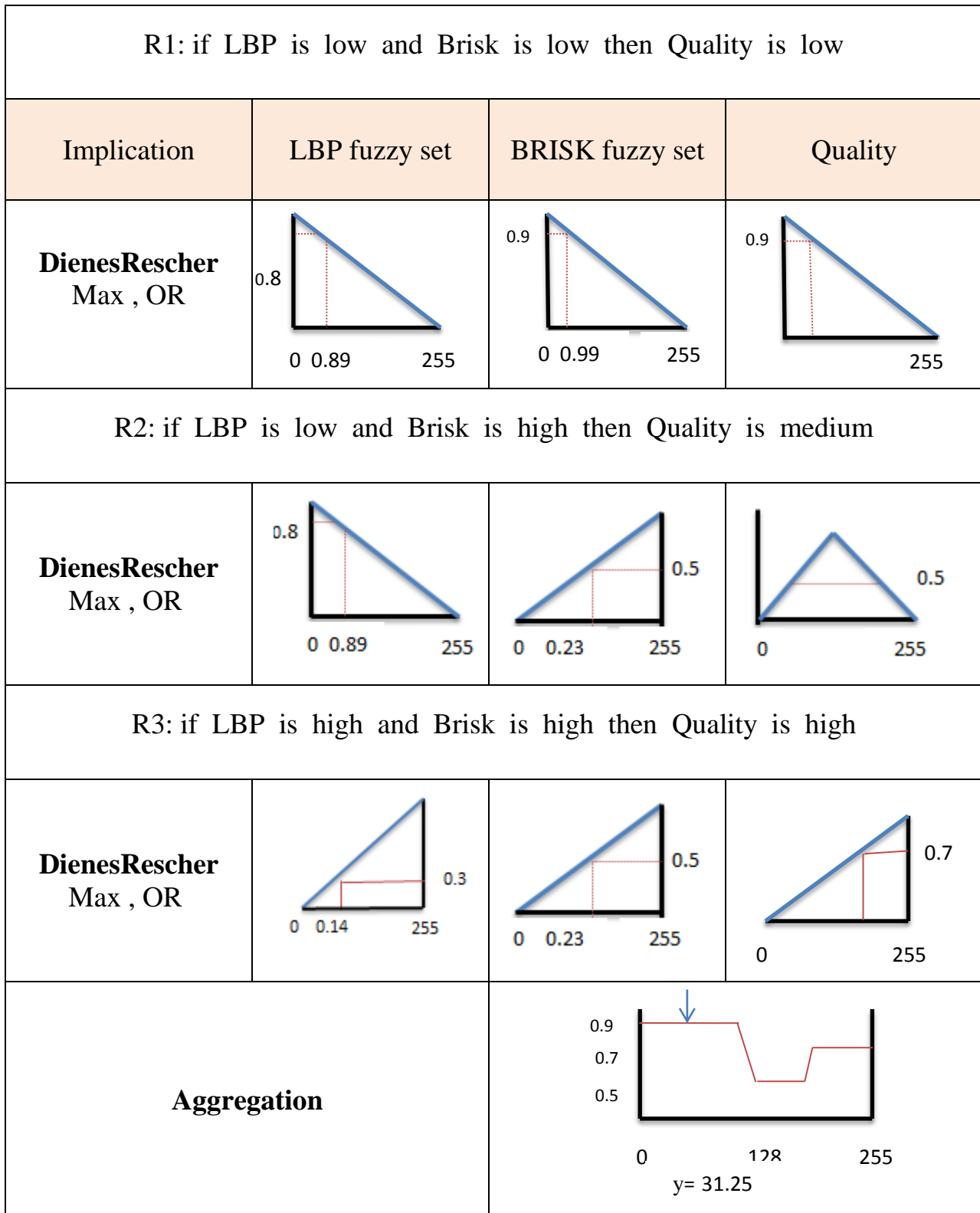


Figure (4.8): Part of the Inference Rule(DienesRescher)

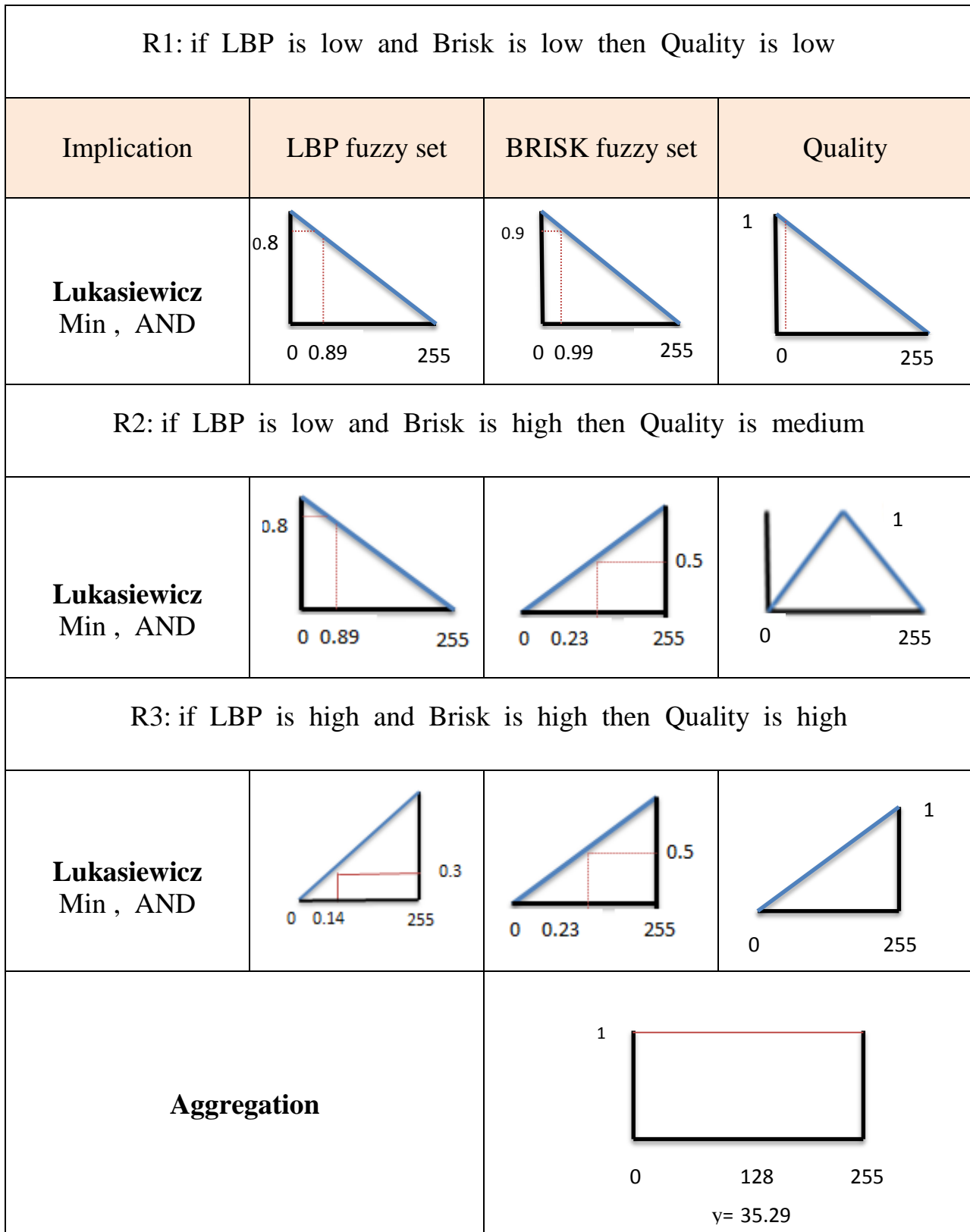


Figure (4.9): Part of the Inference Rule(Lukasiewicz)

Table(4.7) The Features Extraction by Rule Result

	IMP Larsen	IMP Zadeh	IMP DienesRescher	IMP Lukasiewicz	IMP Mamdani
1	0.397	15.420	15.420	3.809	19.230
2	0.106	5.172	5.211	0.596	5.656
3	0.087	4.430	4.579	0.803	4.789
4	0.028	1.670	1.670	0.771	0.898
5	0.031	1.927	1.941	0.602	1.288
6	0.046	2.698	2.771	0.086	2.396
7	0.033	2.007	2.007	0.597	1.410
8	0.079	2.599	3.866	3.542	2.346
9	0.019	1.676	1.676	0.668	1.016
10	0.111	3.870	3.873	0.139	4.002

In Table (4. 7) for any given column represented by the inference operation like Larsen, Zada, , DienesRescher, Lukasiewicz and Mamdani.

Each entry is the result of the relation among corresponding value for five extracted features by the LBP, Surf, Brisk, Harries, and Minengin.

In other words, each output value is computed based on the 5- decision variable to produce the right concluded result. It is a fundamental of fuzzy inference system which enables the approximate reasoning relating multivariate logic.

The computed value is more accurate to be used for classification by PNN rather than using a single feature that would not give the required accuracy.

4.3.2.3 PNN Classifier Implementation

PNN was used to classify data (Magnetic Resonance Imaging of the brain) and classify it into normal and abnormal. Following are the details of this model.

a. Data set construction

The data set were generated based on the input image data set by applying the process of feature extraction and FIS. The result of the data set is shown in Table (4.7). A total of (160- features) had been extracted, based on the total number of images (320) where they divided in to(32- sets), each with (10- images). Then each set produce (5- features) getting totally $[(32*5) = 160]$ features. Again, the (32 sets) consisting of (18 sets) for normal image and (14 sets) for an abnormal image. To get the normal feature , compute $[(32*18) = 90]$ and for abnormal $[(32*14) = 70]$. Table(4.8) gives the training and testing percentage.

Table(4.8) The Number of Features Extracted in Fuzzy Rule

	Total Features	Normal Features	Abnormal Features
Total	160	90	70
Training	112	63	49
Testing	48	27	21

b. Training

1. Impact of the size of training/testing data set.

Table (4.9) illustrated the training /testing percentage and the gained accuracy with total elapsed time in second when the smoothing parameter is constant =0.2 .

Table(4.9) Training /Testing Percentage with Accuracy

Train/Test data set	Number of sample	Accuracy%	Time/second
50% - 50%	80 – 80	93.75	0.41
60% - 40%	96 – 64	93.75	0.47
70% - 30%	112 – 48	100	0.54
80% - 20%	128 – 32	100	0.54
90% - 10%	144 – 16	100	0.55

As shown in the table, this percentage gave a high accuracy of up to 100% plus a short implementation time compared to other rates so that the model based on PNN is fast The classifier can be retrained efficiently in addition to the speed PNN learning gives the ability to adapt real-time learning, as any deletion or addition of training data created in new circumstances.

2- Impact of value smoothing parameter

The effect of the value of the smoothing parameter when data set size is constant 70/30

Table(4.10) Smoothing Parameter Value Impact

Smoothing Parameter	Accuracy %	Train/Test data set
0.1-0.5	100	70% - 30%
0.75	96.875	70% - 30%
1	96.775	70% - 30%
2	96.875	70% - 30%
6	81.25	70% - 30%

The smoothing parameter does not have a significant role in affecting the accuracy of the system. The classification rate is as high as 100% due to the quality of the properties used in the proposed system.

c. Classification

The testing data set forwarded to the system and the confusion matrix is given in Table (4.11) and the performance measurement for this matrix is showed in Table (4.12).

Table (4.11) Confusion Matrix for Classification phase

confusion Matrix		Predicated	
		Normal	Abnormal
Actual	Normal	True Positive (TP = 27)	False Negative (FN = 1)
	Abnormal	False Positive (FP = 0)	True Negative (TN = 20)

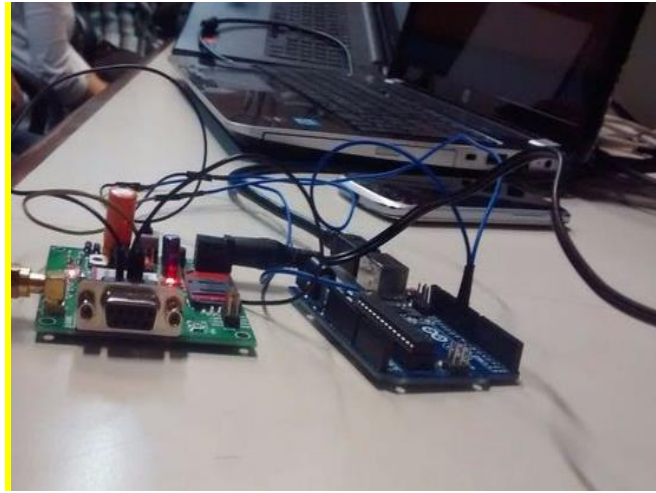
Table(4.12) The Performance Measures for Classification Phase

Sensitivity	0.994
Sepecificity	1
Accuracy	%100
F score	1

The Performance Measures for Classification Phaswere calculated based on Equations No(2.19),(2.20),(2.21) and (2.22).

4.3.3 Transmission Model Implementation:

The Arduino is connected via USB to a computer which acts as a server receives the information related to the final result of the diagnosis, then sends this result via the Global System for Mobile (GSM) by connecting the Arduino unit to GSM via the Arduino pins. After that, the result is sent by the SIM that is connected to the GSM pad by text message to the patient or doctor's phone.



Figure(4.10) Connecting Arduino with Computer and GSM

4.4 Evaluation

In this section, the efficiency of the proposed system was evaluated in terms of accuracy. First, the image registration stage efficiency is compared in Table (4.13) for the population size =10, one generation, and in two cases. In the first case, only the fusion operation is implemented as a crossover operation. In the second case, the wavelet transform followed by fusion was implemented as a crossover operation.

As shown in the table that the entropy value for the combined operation(wavelet followed by fusion) is higher than fusion only, which helps to fast convergence and less number of generation.

Table(4.13) The Entropy of DWT& Fusion

Image 1 Fitness	Image 2 Fitness	Entropy of Fusion	Entropy of Fusion & DWT
1.026	0.987	1.185	5.131
0.957	1.021	1.062	5.084
1.016	0.956	1.097	4.534
0.958	0.906	1.039	4.792
0.987	1.026	1.185	4.789
1.026	0.998	1.131	5.108
0.998	1.021	1.101	4.991
0.987	0.987	0.788	4.938
0.987	0.906	1.128	4.782
0.998	1.021	1.101	4.789

Table (4.14) compares the accuracy of the classification stage with a state of the artwork.

Table(4.14) The PNN and Other Neural Network Accuracy

The sequence	The type of neural network	Accuracy	PNN Accuracy
[11]	PNN	80%	100%
[12]	CNN	97.5%	100%
[15]	CNN	97.75%.	100%

Through this comparison, it indicates that the accuracy ratio of the proposed system is higher than all types of networks used for the same type of image (magnetic resonance imaging) and the same type of case for brain tumors.

4.5 Limitations

- 1- MRI scans have been used exclusively to identify a brain tumor. The system has not been tested on images of another type or other organ in the body.
- 2- The data has not been uploaded to the cloud.

CHAPTER FIVE

CONCLUSIONS AND SUGGESTIONS FOR FUTURE WORK

5.1 Introduction

This chapter includes the conclusions obtained through the implementation of the proposed system. As well as future work recommended by the study.

5.2 Conclusion

Below is an explanation of the conclusions reached through the work:

1. The aim of the works was achieved through the design and implementation of the GA-FL-ANN model for registration and classification of MRI for the brain and automating it via IoT technology (GSM+Arduino).
2. The hybrid system adopted is a cascading style. Outputs for one part are inputs for the next part. This type is characterized by ease of implementation and maintenance.
3. Combine the wavelet transform with the fusion mechanism produces high entropy results for register medical images and speeds up the convergence speed in the GA.
4. Applying the fuzzy logic to combine the feature from feature extraction step is the right choice. It enables to correlate of multiple features at the same time to produce each decision variable; this

increases the accuracy of the classification model and solves the challenge in setting the smooth parameter.

5. PNN is the most appropriate choice for medical image classification since it learn faster. However, its accuracy depends on the feature of the data set and the feature extraction process. The accuracy of proposed system is 100%.

5.3 Suggestion for Future Works

1. Proving the efficiency of the hybrid system by applying it for a less detailed image like CT scans.
2. Using the RNN instead of PNN, and another learning like incremental or iterative learning and compare results.
3. Replacing PNN with a fuzzy neural network or neuron-fuzzy system, and Comparison the results that can be obtained.
4. Automate work across the IoT by uploading data to the cloud for the purpose of preservation and processing.

References

- [1] L. Rundo et al., “MedGA: A novel evolutionary method for image enhancement in medical imaging systems,” *Expert Syst. Appl.*, vol. 119, pp. 387–399, 2019, doi: 10.1016/j.eswa.2018.11.013.
- [2] K. D. Toennies, “Erratum to: Guide to Medical Image Analysis,” pp. E1–E1, 2017, doi: 10.1007/978-1-4471-7320-5_15.
- [3] G. Balakrishnan, A. Zhao, M. R. Sabuncu, J. Guttag, and A. V. Dalca, “VoxelMorph: A Learning Framework for Deformable Medical Image Registration,” *IEEE Trans. Med. Imaging*, vol. 38, no. 8, pp. 1788–1800, Aug. 2019, doi: 10.1109/TMI.2019.2897538.
- [4] M. Bhattacharya and A. Das, “Multimodality medical image registration and fusion techniques using mutual information and genetic algorithm-based approaches,” *Adv. Exp. Med. Biol.*, vol. 696, pp. 441–449, 2011, doi: 10.1007/978-1-4419-7046-6_44.
- [5] S. Karthick and S. Maniraj, “Different Medical Image Registration Techniques: A Comparative Analysis,” *Curr. Med. Imaging Former. Curr. Med. Imaging Rev.*, vol. 15, no. 10, pp. 911–921, Nov. 2019, doi: 10.2174/1573405614666180905094032.
- [6] J. Santamaría, O. Cordón, and S. Damas, “A comparative study of state-of-the-art evolutionary image registration methods for 3D modeling,” *Comput. Vis. Image Underst.*, vol. 115, no. 9, pp. 1340–1354, 2011, doi: 10.1016/j.cviu.2011.05.006.
- [7] P. J. Besl and N. D. McKay, “A Method for Registration of 3-D Shapes,” *IEEE Trans. Pattern Anal. Mach. Intell.*, vol. 14, no. 2, pp. 239–256, 1992, doi: 10.1109/34.121791.
- [8] J. P. W. Pluim, J. B. A. A. Maintz, and M. A. Viergever, “Mutual-information-based registration of medical images: A survey,” *IEEE Trans. Med. Imaging*, vol. 22, no. 8, pp. 986–1004, 2003, doi: 10.1109/TMI.2003.815867.
- [9] A. Das and M. Bhattacharya, “Affine-based registration of CT and MR modality images of human brain using multiresolution approaches: Comparative study on genetic algorithm and particle swarm optimization,” *Neural Comput. Appl.*, vol. 20, no. 2, pp. 223–237, 2011, doi: 10.1007/s00521-010-0374-8.
- [10] L. Ramirez, N. G. Durdle, and V. J. Raso, “Medical image registration in

- computational intelligence framework: A review,” *Can. Conf. Electr. Comput. Eng.*, vol. 2, pp. 1021–1024, 2003, doi: 10.1109/ccece.2003.1226069.
- [11] F. P. M. Oliveira and J. M. R. S. Tavares, “Medical image registration: A review,” *Comput. Methods Biomech. Biomed. Engin.*, vol. 17, no. 2, pp. 73–93, 2014, doi: 10.1080/10255842.2012.670855.
- [12] “Detection of Brain Tumors using Neural Networks.” https://ejmcm.com/article_1812.html (accessed May 28, 2021).
- [13] A. Kabir Anaraki, M. Ayati, and F. Kazemi, “Magnetic resonance imaging-based brain tumor grades classification and grading via convolutional neural networks and genetic algorithms,” *Biocybern. Biomed. Eng.*, vol. 39, no. 1, pp. 63–74, Jan. 2019, doi: 10.1016/j.bbe.2018.10.004.
- [14] B. Heim, F. Krismer, R. De Marzi, and K. Seppi, “Magnetic resonance imaging for the diagnosis of Parkinson’s disease,” *Journal of Neural Transmission*, vol. 124, no. 8. Springer-Verlag Wien, pp. 915–964, Aug. 01, 2017, doi: 10.1007/s00702-017-1717-8.
- [15] H. Zhang, X. Zhou, J. Sun, and J. Zhang, “A novel medical image registration method based on mutual information and genetic algorithm,” *Proc. Conf. Comput. Graph. Imaging Vis. New Trends 2005*, vol. 2005, pp. 221–226, 2005, doi: 10.1109/CGIV.2005.8.
- [16] C. Paulson, S. Ezekiel, and D. Wu, “Wavelet-based image registration,” *Evol. Bio-Inspired Comput. Theory Appl. IV*, vol. 7704, p. 77040M, 2010, doi: 10.1117/12.851210.
- [17] M. Deshmukh and S. Gahankari, “CCIS 147 - Wavelet Transform Based Image Registration and Image Fusion,” pp. 55–60.
- [18] Y. F. Yang, P. X. Wang, J. Li, X. R. Wang, and B. Li, “Medical image registration based on simplified multiwavelet transform,” *Appl. Mech. Mater.*, vol. 513–517, pp. 2739–2743, 2014, doi: 10.4028/www.scientific.net/AMM.513-517.2739.
- [19] B. Deepa, M. G. Sumithra, T. D. Bharathi, and S. Rajesh, “MRI Medical Image Fusion Using Gradient Based Discrete Wavelet Transform,” *2017 IEEE Int. Conf. Comput. Intell. Comput. Res. ICCIC 2017*, pp. 1–4, 2018, doi: 10.1109/ICCIC.2017.8524436.
- [20] R. Lavanyadevi, M. MacHakowsalya, J. Nivethitha, and A. Niranjil Kumar, “Brain tumor classification and segmentation in MRI images using PNN,” in *Proceedings - 2017 IEEE International Conference on Electrical,*

- Instrumentation and Communication Engineering, ICEICE 2017, Dec. 2017, vol. 2017-Decem, pp. 1–6, doi: 10.1109/ICEICE.2017.8191888.
- [21] J. Seetha and S. S. Raja, “Brain tumor classification using Convolutional Neural Networks,” *Biomed. Pharmacol. J.*, vol. 11, no. 3, pp. 1457–1461, 2018, doi: 10.13005/bpj/1511.
- [22] H. Mohsen, E.-S. A. El-Dahshan, E.-S. M. El-Horbaty, and A.-B. M. Salem, “Classification using deep learning neural networks for brain tumors,” *Futur. Comput. Informatics J.*, vol. 3, no. 1, pp. 68–71, 2018, doi: 10.1016/j.fcij.2017.12.001.
- [23] H. Ucuzal, S. Yasar, and C. Colak, “Classification of brain tumor types by deep learning with convolutional neural network on magnetic resonance images using a developed web-based interface,” Oct. 2019, doi: 10.1109/ISMSIT.2019.8932761.
- [24] C. Gungen, O. Polat, and R. Karakis, “Classification of Brain Tumors using Convolutional Neural Network from MR Images,” Oct. 2020, doi: 10.1109/SIU49456.2020.9302090.
- [25] K. Dagli and O. Erogul, “Classification of Brain Tumors via Deep Learning Models,” Nov. 2020, doi: 10.1109/TIPTEKNO50054.2020.9299231.
- [26] G. Song, J. Han, Y. Zhao, Z. Wang, and H. Du, “A Review on Medical Image Registration as an Optimization Problem,” *Curr. Med. Imaging Rev.*, vol. 13, no. 3, pp. 274–283, 2017, doi: 10.2174/1573405612666160920123955.
- [27] B. Zitová and J. Flusser, “Image registration methods: A survey,” *Image Vis. Comput.*, vol. 21, no. 11, pp. 977–1000, 2003, doi: 10.1016/S0262-8856(03)00137-9.
- [28] J. Ker, L. Wang, J. Rao, and T. Lim, “Deep Learning Applications in Medical Image Analysis,” *IEEE Access*, vol. 6, pp. 9375–9379, Dec. 2017, doi: 10.1109/ACCESS.2017.2788044.
- [29] B. J. Erickson and C. R. Jack, “Correlation of single photon emission CT with MR image data using fiduciary markers,” *Am. J. Neuroradiol.*, vol. 14, no. 3, 1993.
- [30] M. A. Ibrahim and A. B. Dublin, *Magnetic Resonance Imaging (MRI), Gadolinium*. StatPearls Publishing, 2018.
- [31] R. Fusco et al., “Magnetic resonance imaging evaluation in neoadjuvant therapy of locally advanced rectal cancer: A systematic review,” *Radiology and*

- Oncology, vol. 51, no. 3. Association of Radiology and Oncology, pp. 252–262, Aug. 16, 2017, doi: 10.1515/raon-2017-0032.
- [32] S. R. Cherry, R. D. Badawi, J. S. Karp, W. W. Moses, P. Price, and T. Jones, “Total-body imaging: Transforming the role of positron emission tomography,” *Science Translational Medicine*, vol. 9, no. 381. American Association for the Advancement of Science, Mar. 15, 2017, doi: 10.1126/scitranslmed.aaf6169.
- [33] C. Michail et al., “A novel method for the optimization of positron emission tomography scanners imaging performance,” *Hell. J. Nucl. Med.*, vol. 19, no. 3, pp. 231–240, Sep. 2016, doi: 10.1967/s002449910405.
- [34] M. Mozaffarzadeh, M. Sadeghi, A. Mahloojifar, and M. Orooji, “Double-Stage Delay Multiply and Sum Beamforming Algorithm Applied to Ultrasound Medical Imaging,” *Ultrasound Med. Biol.*, vol. 44, no. 3, pp. 677–686, Mar. 2018, doi: 10.1016/j.ultrasmedbio.2017.10.020.
- [35] H. Khalid et al., “A Comparative Systematic Literature Review on Knee Bone Reports from MRI, X-Rays and CT Scans Using Deep Learning and Machine Learning Methodologies,” *Diagnostics*, vol. 10, no. 8, p. 518, Jul. 2020, doi: 10.3390/diagnostics10080518.
- [36] M. Norouzi, G. Akbarizadeh, and F. Eftekhari, “A hybrid feature extraction method for SAR image registration,” *Signal, Image Video Process.*, vol. 12, no. 8, pp. 1559–1566, Nov. 2018, doi: 10.1007/s11760-018-1312-y.
- [37] S. Chelbi and A. Mekhmoukh, “Features based image registration using cross correlation and Radon transform,” *Alexandria Eng. J.*, vol. 57, no. 4, pp. 2313–2318, Dec. 2018, doi: 10.1016/j.aej.2017.07.013.
- [38] C. Silva, T. Bouwmans, and C. Frélicot, “An extended center-symmetric local binary pattern for background modeling and subtraction in videos,” in *VISAPP 2015 - 10th International Conference on Computer Vision Theory and Applications; VISIGRAPP, Proceedings*, Mar. 2015, vol. 1, pp. 395–402, doi: 10.5220/0005266303950402.
- [39] M. S. Nixon and A. S. Aguado, *Feature extraction and image processing for computer vision*. 2019.
- [40] M. S. Patel, N. M. Patel, and M. S. Holia, “Feature based multi-view image registration using SURF,” in *2015 International Symposium on Advanced Computing and Communication, ISACC 2015*, Jan. 2016, pp. 213–218, doi: 10.1109/ISACC.2015.7377344.
- [41] R. Y. S. Leutenegger Stefan, Margarita Chli, “BRISK: Binary robust invariant

- scalable keypoints.’ Computer Vision (ICCV),” *Iccv*, pp. 2548–2555, 2011.
- [42] J. B. Ryu, C. G. Lee, and H. H. Park, “Formula for Harris corner detector,” *Electron. Lett.*, vol. 47, no. 3, pp. 180–181, Feb. 2011, doi: 10.1049/el.2010.3403.
- [43] P. Ram and S. Padmavathi, “Analysis of Harris corner detection for color images,” in *International Conference on Signal Processing, Communication, Power and Embedded System, SCOPES 2016 - Proceedings*, Jun. 2017, pp. 405–410, doi: 10.1109/SCOPES.2016.7955862.
- [44] W. Peng, X. Hongling, L. Wenlin, and S. Wenlong, “Harris Scale Invariant Corner Detection Algorithm Based on the Significant Region,” *Int. J. Signal Process. Image Process. Pattern Recognit.*, vol. 9, no. 3, pp. 413–420, 2016, doi: 10.14257/ijcip.2016.9.3.35.
- [45] G. Wang, C. Lopez-Molina, and B. De Baets, “Multiscale Edge Detection Using First-Order Derivative of Anisotropic Gaussian Kernels,” *J. Math. Imaging Vis.*, vol. 61, no. 8, pp. 1096–1111, Oct. 2019, doi: 10.1007/s10851-019-00892-1.
- [46] C. Science, L. G. Kabari, K. S. Polytechnic, P. Day, and I. Design, “A Spatial Domain for Image Enhancement using Gaussian Filter,” no. March, 2020, doi: 10.24214/jecet.B.9.1.
- [47] A. de Juan, A. Gowen, L. Duponchel, and C. Ruckebusch, *Image Fusion*, vol. 31. 2019.
- [48] H. Kaur, D. Koundal, and V. Kadyan, “Image Fusion Techniques: A Survey,” *Arch. Comput. Methods Eng.*, no. 0123456789, 2021, doi: 10.1007/s11831-021-09540-7.
- [49] F. C. Morabito, G. Simone, and M. Cacciola, “Image fusion techniques for non-destructive testing and remote sensing applications,” in *Image Fusion*, Elsevier, 2008, pp. 367–392.
- [50] Z. Wang, D. Ziou, C. Armenakis, D. Li, and Q. Li, “A Comparative Analysis of Image Fusion Methods,” vol. 43, no. 6, pp. 1391–1402, 2005.
- [51] C. Cai and P. D. B. Harrington, “Different discrete wavelet transforms applied to denoising analytical data,” *J. Chem. Inf. Comput. Sci.*, vol. 38, no. 6, pp. 1161–1170, 1998, doi: 10.1021/ci980210j.
- [52] M. B. Abdulkareem, “Design and Development of Multimodal Medical Image Fusion using Discrete Wavelet Transform,” in *Proceedings of the International*

- Conference on Inventive Communication and Computational Technologies, ICICCT 2018, Sep. 2018, pp. 1629–1633, doi: 10.1109/ICICCT.2018.8472997.
- [53] V. Nežerka and J. Trejbal, “Assessment of aggregate-bitumen coverage using entropy-based image segmentation,” *Road Mater. Pavement Des.*, vol. 21, no. 8, pp. 2364–2375, Nov. 2020, doi: 10.1080/14680629.2019.1605304.
- [54] D. Y. Tsai, Y. Lee, and E. Matsuyama, “Information entropy measure for evaluation of image quality,” *J. Digit. Imaging*, vol. 21, no. 3, pp. 338–347, Sep. 2008, doi: 10.1007/s10278-007-9044-5.
- [55] B. S. Min, D. K. Lim, S. J. Kim, and J. H. Lee, “A novel method of determining parameters of CLAHE based on image entropy,” *Int. J. Softw. Eng. its Appl.*, vol. 7, no. 5, pp. 113–120, 2013, doi: 10.14257/ijseia.2013.7.5.11.
- [56] L. A. Zadeh, “Soft Computing and Fuzzy Logic,” *IEEE Softw.*, vol. 11, no. 6, pp. 48–56, 1994, doi: 10.1109/52.329401.
- [57] G. Ruiz-Garcia, H. Hagrais, H. Pomares, and I. R. Ruiz, “Toward a Fuzzy Logic System Based on General Forms of Interval Type-2 Fuzzy Sets,” *IEEE Trans. Fuzzy Syst.*, vol. 27, no. 12, pp. 2381–2395, Dec. 2019, doi: 10.1109/TFUZZ.2019.2898582.
- [58] A. Mardani et al., “Application of decision making and fuzzy sets theory to evaluate the healthcare and medical problems: A review of three decades of research with recent developments,” *Expert Syst. Appl.*, vol. 137, pp. 202–231, 2019, doi: 10.1016/j.eswa.2019.07.002.
- [59] R. R. Yager, “Generalized Orthopair Fuzzy Sets,” *IEEE Trans. Fuzzy Syst.*, vol. 25, no. 5, pp. 1222–1230, Oct. 2017, doi: 10.1109/TFUZZ.2016.2604005.
- [60] G. Qingrong, J. Zhenhong, Y. Jie, and N. Kasabov, “Contrast enhancement of medical images using fuzzy set theory and nonsubsampling shearlet transform,” *Int. J. Imaging Syst. Technol.*, vol. 29, no. 4, pp. 483–490, 2019, doi: 10.1002/ima.22326.
- [61] M. Miralinaghi, Y. Lou, Y. T. Hsu, R. Shabanpour, and Y. Shafahi, “Multiclass fuzzy user equilibrium with endogenous membership functions and risk-taking behaviors,” *J. Adv. Transp.*, vol. 50, no. 8, pp. 1716–1734, 2016, doi: 10.1002/atr.1425.
- [62] Imoh J. Eyoh and 1Uduak A. Umoh, “A Comparative Analysis of Fuzzy Inference Engines in Context of Profitability Control,” *J. Adv. Transp.*, Vol. 24 No. 7 (2014).

- [63] Y. Bai and D. Wang, “Fundamentals of Fuzzy Logic Control — Fuzzy Sets, Fuzzy Rules and Defuzzifications BT - Advanced Fuzzy Logic Technologies in Industrial Applications,” pp. 17–36, 2006.
- [64] P. Hajek and V. Olej, “Defuzzification methods in intuitionistic fuzzy inference systems of Takagi-Sugeno type: The case of corporate bankruptcy prediction,” 2014 11th Int. Conf. Fuzzy Syst. Knowl. Discov. FSKD 2014, pp. 232–236, 2014, doi: 10.1109/FSKD.2014.6980838.
- [65] T. Talaška, “Components of artificial neural networks realized in CMOS technology to be used in intelligent sensors in wireless sensor networks,” *Sensors (Switzerland)*, vol. 18, no. 12, 2018, doi: 10.3390/s18124499.
- [66] A. Kun et al., “Number 912 Network traffic classification via neural networks Network Traffic Classification via Neural Networks,” 2017, Accessed: Dec. 14, 2020.
- [67] Y. Zeinali and B. A. Story, “Competitive probabilistic neural network,” *Integr. Comput. Aided. Eng.*, vol. 24, no. 2, pp. 105–118, Jan. 2017, doi: 10.3233/ICA-170540.
- [68] D. F. Specht and H. Romsdahl, “Experience with adaptive probabilistic neural networks and adaptive general regression neural networks,” in *IEEE International Conference on Neural Networks - Conference Proceedings*, 1994, vol. 2, pp. 1203–1212, doi: 10.1109/icnn.1994.374355.
- [69] M. Zhong et al., “Gap-based estimation: Choosing the smoothing parameters for probabilistic and general regression neural networks,” *IEEE Int. Conf. Neural Networks - Conf. Proc.*, pp. 1870–1877, 2006, doi: 10.1109/ijcnn.2006.246908.
- [70] M. Zhong et al., “Probabilistic Neural Network: Comparisons of the Cross-Validation Approach and a Fast Heuristic to choose the Smoothing Parameters,” *Artif. Neural Networks Eng.*, pp. 1–10, 2005.
- [71] H. Farhidzadeh, “Probabilistic Neural Network Training for Semi-Supervised Classifiers,” pp. 461–474, 2015.
- [72] D. Jude Hemanth and J. Anitha, “Modified Genetic Algorithm approaches for classification of abnormal Magnetic Resonance Brain tumour images,” *Appl. Soft Comput. J.*, vol. 75, pp. 21–28, 2019, doi: 10.1016/j.asoc.2018.10.054.
- [73] V. T. Ingole, C. N. Deshmukh, A. Joshi, and D. Shete, “Medical image registration using genetic algorithm,” in *2009 2nd International Conference on Emerging Trends in Engineering and Technology, ICETET 2009*, 2009, pp.

- 63–66, doi: 10.1109/ICETET.2009.143.
- [74] K. R. Hole, V. S. Gulhane, and N. D. Shellokar, “Application of Genetic Algorithm for Image Enhancement and Segmentation .,” *Int. J. Adv. Res. Comput. Eng. Technol.*, vol. 2, no. 4, pp. 1342–1346, 2013.
- [75] L. Altenberg, “Evolutionary Computation,” *Encycl. Evol. Biol.*, pp. 40–47, 2016, doi: 10.1016/B978-0-12-800049-6.00307-3.
- [76] N. M. Razali and J. Geraghty, “Genetic algorithm performance with different selection strategies in solving TSP,” *Proc. World Congr. Eng. 2011, WCE 2011*, vol. 2, pp. 1134–1139, 2011.
- [77] S. Mirjalili, “Genetic algorithm,” *Stud. Comput. Intell.*, vol. 780, pp. 43–55, 2019, doi: 10.1007/978-3-319-93025-1_4.
- [78] A. Hussain, Y. S. Muhammad, M. Nauman Sajid, I. Hussain, A. Mohamd Shoukry, and S. Gani, “Genetic Algorithm for Traveling Salesman Problem with Modified Cycle Crossover Operator,” *Comput. Intell. Neurosci.*, vol. 2017, 2017, doi: 10.1155/2017/7430125.
- [79] S. C. Techniques, “Note (Soft Computing).” Book.
- [80] Z. Lai and H. Deng, “Medical image classification based on deep features extracted by deep model and statistic feature fusion with multilayer perceptron,” *Comput. Intell. Neurosci.*, vol. 2018, 2018, doi: 10.1155/2018/2061516.
- [81] Y. Xu, L. Li, J. Ding, L. Y. Wu, G. Mai, and F. Zhou, “Gly-PseAAC: Identifying protein lysine glycation through sequences,” *Gene*, vol. 602, pp. 1–7, Feb. 2017, doi: 10.1016/j.gene.2016.11.021.
- [82] “C Programming For the PC the MAC and the Arduino Microcontroller System - Peter”. Author House%2C 2013&f=false (accessed Dec. 24, 2020).
- [83] Y. A. Badamasi, “The working principle of an Arduino,” *Proc. 11th Int. Conf. Electron. Comput. ICECCO 2014*, 2014, doi: 10.1109/ICECCO.2014.6997578.
- [84] L. Louis, “Working Principle of Arduino and Using it as a Tool for Study and Research,” *Int. J. Control. Autom. Commun. Syst.*, vol. 1, no. 2, pp. 21–29, 2016, doi: 10.5121/ijcacs.2016.1203.
- [85] B. I. Bakare, I. A. Ekanem, and I. O. Allen, “Appraisal of Global System for Mobile Communication (GSM) In Nigeria American Journal of Engineering Research (AJER),” no. 6, pp. 97–102, 2017.

- [86] T. H. Nasution, M. A. Muchtar, I. Siregar, U. Andayani, E. Christian, and E. P. Sinulingga, “Electrical appliances control prototype by using GSM module and Arduino,” 2017 4th Int. Conf. Ind. Eng. Appl. ICIEA 2017, pp. 355–358, 2017, doi: 10.1109/IEA.2017.7939237.

الخلاصة

تطور التكنولوجيا له أهمية كبيرة في الحياة ، في أي مكان وفي الوقت الحاضر ، تبرز تلك الأهمية في مجال الرعاية الصحية بشكل ملحوظ. والتي تساهم في التشخيص التلقائي للأمراض بدقة وكفاءة عالية ووقت أقل. تلعب أنظمة التصوير الطبي دورًا رئيسيًا في سير العمل السريري لقدرتها على عكس السمات التشريحية والفسيولوجية التي يتعذر الوصول إليها للفحص يُعد التنبؤ بأمراض الدماغ ومدى تسلل الخلايا السرطانية والكشف عنها أهم قضية في سير عمل الأتمتة السريرية. تكون بحاجة إلى خطوة معالجة مسبقة لتحليل الصور بدقة عالية.

يعتبر تسجيل الصورة الطبية أكثر خطوات المعالجة المسبقة ملائمة في تحليل الصور ومحاذاتها في أوقات مختلفة من مصادر مختلفة وفي ظروف تصوير مختلفة ، بالإضافة إلى ذلك يمكن الحصول على صورة متكاملة الخصائص عن طريق دمج صورتين. العديد من الأبحاث والدراسات السابقة اقترحت تقنيات مختلفة في تسجيل الصور الطبية ، والتشخيص الطبي لكن عدم تكامل الكفاءة ودقة التسجيل وقلة الشمولية ، كالاقتصار على نوع معين من الصور ، أو حجم معين ، بالإضافة إلى تعقيد الخوارزمية المستخدمة ومسألة الوقت ، أو قد لا يكون هناك تحسين. تعتبر نقاط الضعف في تلك الدراسات.

في هذه الأطروحة ، يهدف هذا العمل إلى تطوير نموذج الحوسبة الناعمة لتسجيل الصور كمرحلة أولى في نظام التشخيص الآلي. حيث تم اقتراح نظام هجين لتسجيل التصوير بالرنين المغناطيسي للدماغ بناءً على الخوارزمية الجينية التي تضم التحويل الموجي والاندماج للحصول على نتائج أكثر دقة. ثم استخدام نموذج ضبابي كجسر بين مرحلة MIR وكشف الصورة للتعامل مع الغموض في بيانات الصورة. أخيراً مرحلة الكشف والتشخيص التي تبنى على أساس PNN يتم ذلك بالاعتماد على الشبكة الخلوية التي تتيح أتمتة التشخيص في العيادة أشارت النتائج التجريبية إلى أن النظام المقترح يتمتع بمتوسط معدل دقة مرتفع مقارنة بالطرق الأخرى الموجودة حيث يبلغ متوسط الدقة (100%) باستخدام PNN ويمكن اعتماده كنظام تشخيص مؤتمت.



وزارة التعليم العالي والبحث العلمي

الجامعة العراقية

كلية الهندسة / قسم هندسة الحاسوب



نموذج الحوسبة المرنة لتسجيل الصور وتصنيفها: دراسة حالة أوران الدماغ

أطروحة

مقدمة لكلية الهندسة في الجامعة العراقية في استيفاء جزئي لمتطلبات درجة
ماجستير العلوم في هندسة الحاسوب

بواسطة

إسراء يعرب يوسف عبد الحسين

المشرف

استاذ مساعد. دكتور. تيسير سلمان عطية

استاذ مساعد. دكتور. مشتاق احمد علي